CHARLES UNIVERSITY

FACULTY OF PHARMACY IN HRADEC KRÁLOVÉ

Department of Pharmaceutical Chemistry and Pharmaceutical Analysis

SYNTHESIS OF NOVEL INHIBITORS OF HUMAN TOPOISOMERASE BASED ON HIGHLY SUBSTITUTED PHENYL SCAFFOLD

DIPLOMA THESIS

Miroslav Domanský

Supervisor: doc. PharmDr. Jan Zitko, Ph,D.

Consultant: Mgr. Marek Kerda

Hradec Králové 2023

This work was performed during Erasmus+ stay in:

University of Ljubljana

Faculty of Pharmacy

Department of Pharmaceutical Chemistry

Under the supervision of:

Prof. Janez Ilaš, M. Pharm., Ph.D.

And revised in:

Charles University

Faculty of Pharmacy in Hradec Králové

Department of Pharmaceutical Chemistry and Pharmaceutical Analysis

Under the supervision of:

doc. PharmDr. Jan Zitko, Ph.D.

Mgr. Marek Kerda

„Prohlašuji, že tato práce je mým původním autorským dílem. Veškerá literatura a další zdroje, z nichž jsem při zpracování čerpal, jsou uvedeny v seznamu použité literatury a v práci řádně citovány. Práce nebyla využita k získání jiného nebo stejného titulu.“

“I declare that this thesis is my original author’s work. Literature and other resources used were in-text cited and referenced accordingly. The work has not been submitted to obtain the same or another title.”

Miroslav Domanský

Hradec Králové, August 2023

Acknowledgement

I want to thank Prof. Janez Ilaš, M. Pharm., Ph.D. immensely for allowing me to participate in this project at the Department of Pharmaceutical Chemistry at the University of Ljubljana and for supervising me during my Erasmus+ stay in Ljubljana. My sincere gratitude also goes to my supervisor doc. PharmDr. Jan Zitko, Ph.D. for help with this project.

Special thanks go to my consultant Mgr. Marek Kerda, who kindly and with patience guided me in the laboratory at the Faculty of Pharmacy in Hradec Králové over the years, gave me valuable advice and helped me to put together numerous projects and this thesis.

I would like to acknowledge the assistance of Ilaria Brau, M. Pharm., who shared her practical laboratory experience and protocols with me during my Erasmus+ stay.

Lastly, I would like to thank all the master´s students, Ph.D. students, assistants, and researchers with whom I shared the laboratory.

This work was supported by the Ministry of Education, Youth and Sports of the Czech Republic (project SVV 260 666) and by the Erasmus + project of Charles University.

Table of contents

Abstract 8

Abstrakt 9

Abbreviations 10

1. Aim of work 12

2. Theoretical part 13

2.1 Introduction 13

2.2 What cancer is 13

2.3 Topoisomerases 14

2.3.1 Topoisomerase I 16

2.3.2 Topoisomerase II 17

2.4 Inhibitors of DNA topoisomerases 18

2.4.1 Inhibitors of Topoisomerase I 18

2.4.2 Inhibitors of Topoisomerase II 20

2.4.2.1 TopoII poisons 20

2.4.2.2 Catalytic inhibitors 21

2.5 Structure-activity relationship 22

3. Experimental part 26

3.1 Synthesis of IMD 0 series - Complete reaction scheme 26

3.1.1 Synthesis of IMD-01 27

3.1.2 Synthesis of IMD-02 28

3.1.3 Synthesis of IMD-03 29

3.1.4 Synthesis of IMD-04 31

3.2 Synthesis of IMD 1 series – complete reaction scheme 32

3.2.1 Synthesis of IMD-11 33

3.2.2 Synthesis of IMD-12 34

3.2.3 Synthesis of IMD-13 35

3.3 Synthesis of IMD 2 series – complete reaction scheme of starting material ..36
3.3.1 Synthesis of IMD-21 ..36
3.3.2 Synthesis of IMD-22 ..37
3.4 Synthesis of IMD 2 series – complete reaction scheme of the first derivate ..38
3.4.1 Synthesis of IMD-23a ..39
3.5 Synthesis of IMD 2 series – complete reaction scheme of the second derivate.43
3.5.1 Synthesis of IMD-24a ..44
3.5.2 Synthesis of IMD-24b ..45
3.5.3 Synthesis of IMD-24c ..46
3.6 Synthesis of IMD 2 series – complete reaction scheme of the third derivate .48
3.6.1 Synthesis of IMD-25a ..49
3.6.2 Synthesis of IMD-25b ..51
3.7 Compounds' characterizations ..52
3.7.1 IMD-01 ..53
3.7.2 IMD-02 ..54
3.7.3 IMD-03 ..55
3.7.4 IMD-04 ..56
3.7.5 IMD-11 ..58
3.7.6 IMD-12 ..59
3.7.7 IMD-21 ..60
3.7.8 IMD-22 ..61
3.7.9 IMD-24a ..62
3.7.10 IMD-24b ..64
3.7.11 IMD-25a ..66
3.7.12 IMD-25b ..67
4. Methods ..68
4.1 General and instrumentation ..68

4.2 Topoisomerase IIα inhibition assay 69
5. Results & discussion 70
6. Conclusion 71
7. Literature 72

Abstract

Despite progress in anticancer therapy, cancer is still one of the leading causes of death in the world. Patients treated with current anticancer therapy suffer from many side effects. This is caused by the low selectivity of the current drugs. The development of chemotherapeutics aims to prepare more selective and therefore better tolerated anticancer drugs.

Topoisomerases are nuclear enzymes occurring in every cell. They have an essential role – to preserve DNA and repair it. Topoisomerase isoform IIα is an isoform that controls and edits the conformation of DNA during cell replication. Its expression is highly elevated in proliferating cells. That makes it a good target for anticancer drugs.

The design of synthesized molecules is based on previously reported ATP-competitive inhibitors of human topoisomerase IIα. Alterations of 3,4-dichloro-5-methyl-*N*-phenyl-1*H*-pyrrole-2-carboxamide have been synthesized based on Computational-Aided Drug Design. The *in silico* study is based on the previous discovery of the ATP cavity biding pattern. It was found that halogen-substituted pyrrole-2-carboxamide moiety is crucial for the inhibition of the target.

This project aimed to synthesize novel inhibitors of topoisomerase IIα. Synthesized compounds were tested for inhibitory activity and the IC_{50} on hTopoII is 25 μM. Further details of synthesis and biological evaluations will be discussed in the thesis.

Abstrakt

Navzdory pokroku v léčbě rakoviny je toto onemocnění jednou z vedoucích příčin úmrtí na světě. Pacienti léčeni protirakovinovou léčbou často trpí mnoha nežádoucími účinky této léčby. To je způsobeno nízkou selektivitou současných léčiv. Cílem vývoje nových léčiv proti rakovině je připravit více selektivní a lépe snášená léčiva.

Topoisomerázy jsou jaderné enzymy vyskytující se v každé buňce lidského těla. Jejich funkcí je zachovávat a opravovat DNA. α isoforma topoisomerázy II kontroluje a případně upravuje konformaci DNA během buněčného dělení. Její vysoké hladiny se vyskytují ve vysoce proliferujících buňkách, což z ní dělá dobrý cíl pro protinádorovou léčbu.

Design syntetizovaných molekul je založen na dříve publikovaných ATP-kompetitivních inhibitorech lidské topoisomerázy IIα. Obměny 3,4-dichloro-5-metyl-N-fenyl-1*H*-pyrol-2-karboxamidu byly syntetizovány na základě počítačem podporovaného designu léčiv. *In silico* studie vychází z dříve publikovaných objevů vazebného motivu do ATP kavity. Bylo objeveno, že halogenem substituovaný pyrol-2-karboxamidový fragment je pro inhibiční aktivitu nezbytný.

Cílem této práce bylo nasyntetizovat nové inhibitory lidské topoisomerázy IIα. U připravených sloučenin byla stanovena inhibiční aktivita vůči hTopoII na 25 μM. Výsledky testování a podrobnosti týkající se syntézy budou blíže probrány v rámci této práce.

Abbreviations

ACN – acetonitrile

ADP – adenosine diphosphate

ATP – adenosine triphosphate

$CDCl_3$ – deuterated chloroform

DCM – dichloromethane

DMSO – dimethylsulfoxide

DMSO-d_6 – deuterated dimethylsulfoxide

DMF – *N,N*-dimethylformamide

EtOAc – ethyl acetate

HepG2 – human liver cancer cell line

Hex - hexane

^{1}H NMR – proton nuclear magnetic resonance

HPLC-MS – high-performance liquid chromatography-mass spectrometry

hTopoI – human topoisomerase I

hTopoII – human topoisomerase II

hTopoIIα – human topoisomerase IIα

hTopoIIβ – human topoisomerase IIβ

IARC – The International Agency for Research on Cancer

IC_{50} – half-maximal inhibitory concentration

MCF-7 – breast cancer cell line

MeOH – methanol

ON – overnight

RT – room temperature

RM – reaction mixture

SM – starting material

S_NAr – nucleophilic aromatic substitution

TEA – triethylamine

TFA – trifluoroacetic acid

TLC – thin-layer chromatography

topoI – topoisomerase I

topoII – topoisomerase II

topoIIα – topoisomerase IIα

topoIIβ – topoisomerase IIβ

UV – ultraviolet

WHO – World Health Organization

1. Aim of work

The design of synthesized compounds is based on previous work done at the University of Ljubljana and they share similar structural patterns with previously synthesized substances (Figure 1).

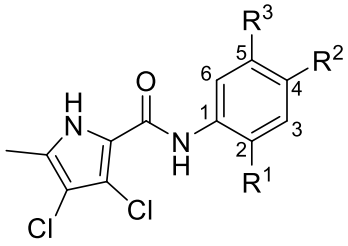

Figure 1 General structure of intended compounds.

Previous hit compounds showed both good on-target and cytotoxic activity. However, they were non-specific to hTopoIIα and they possessed insufficient physicochemical properties. This work aimed to prepare novel derivatives of previously synthesized compounds with improved physicochemical properties and evaluate their inhibitory activity.

Methylsulfonyl group was chosen as substituent in position 5 and benzyloxy moiety was attached in position 2 for the first series of reactions. Compounds with benzothiazole occupying positions 4 and 5 were attempted to synthesize in the second series of reactions.

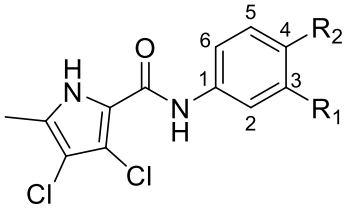

Figure 2 Different pattern for the last reactions.

Substances with different patterns (Figure 2) were attempted to prepare in the last series of reactions. They were substituted by carboxamide in position 4 and by greater moiety, containing a six-atom saturated ring, in position 3.

In contrast with substances synthesized by Skok et al., these structures should form hydrogen bonds in the binding cavity, but at pH 7.4 should be non-ionized.

2. Theoretical part

2.1 Introduction

Cancer is the second leading cause of death in the world according to WHO (10 million in 2020)[1]. Survival rates for many types of cancer are improving (the most common cancers are lung, breast, prostate and colorectal)[2], but as the population grows and ages and diagnostic methods are being improved, the burden of cancer grows[3] (18.1 million new cases in 2018[4], 19.3 million new cases in 2020[1]). Other causes may be related to the nowadays lifestyle, diet, and emotional strain.[2] Key elements for the fight against cancer are targeted screening, early diagnosis, and early treatment.[5] In 1965 World Health Assembly established The International Agency for Research on Cancer (IARC) as an autonomous agency of WHO, which coordinates international collaboration in cancer research trying to find new effective and selective chemotherapeutics.[6]

2.2 What is cancer

There are between 50 to 100 trillion cells in the human body, which form higher building blocks such as tissues and organs. Each of these higher building blocks consists of specialized cells that grow and divide to fulfil the needs of the body.[7] When the healthy cells get old or damaged to the point where the cell´s repair mechanisms fail, they perform apoptosis and die, so new healthy cells can take their place. Sometimes a damaged cell evades the apoptosis.[8] The body has mechanisms to recognize such cells and kill them with the help of the immune system.[9] However, some of such damaged cells can develop the ability to suppress the immune response.[10] This condition is called cancer. Cancer is often named by the organ or tissue of origin; it can also be described by the type of cell that forms it.[11]

Cancer is a huge group of diseases (there are more than 100 known types of cancer) that can affect practically any organ or tissue. It may start anywhere in the body and often results in growing tumours. There are two types of tumours: benign (noncancerous) and malignant (cancerous). Benign tumours grow slowly, do not spread through the body, and therefore do not pose a major life-threatening risk. Malignant tumours tend to grow rapidly, ignore the body´s signals to stop growing, oppress or even destroy surrounding tissues, and in late phases metastasize (travel from one place of origin to another place in the body). Cancer is associated with malignant tumours. [11,12]

Several mutations and/or epigenetic (genetic expression) changes are needed to transform normal cells into malignant.[9] Such cell needs a large amount of nutrients for reproduction and a higher concentration of corresponding enzymes.[13] Enzymes controlling the conformation of DNA are among those essential for cancer cells. These are the enzymes responsible for the fast replication and survival of the cell. Among these enzymes, topoisomerases are important targets for anticancer therapy.[14]

2.3 Topoisomerases

DNA forms higher structures that are necessary for its proper function in the cell. This implies that the conformation of DNA affects replication and transcription and therefore survival of the cell. Many processes in the cell require a specific DNA superstructure, which must be preserved for a certain time. A lot of DNA-dependent acts are accompanied by transient structure tension of DNA molecule, which must be released to restore its functionality. In some cases, DNA also has to be condensed into complex superstructures during certain stages of the cell cycle (e.g. creation of nucleosomes).[15] Utilization of information stored in DNA requires untangling of the superstructure and separation of double helix strands temporarily (transcription or recombination) or permanently (replication).[16]

In the normal state, DNA of the most organisms forms a tertiary structure known as a supercoil. Supercoil is a DNA duplex tangled into tertiary structures by rotation, which can happen in two ways, therefore there are two types of supercoils - negative and positive.[17] DNA of nearly all organisms is negatively supercoiled. It becomes positively supercoiled only during transcription or replication when transcription enzymes generate positive strain on the strand.[18]

The negative supercoiling is a right-handed rotation tangling DNA duplex into counter-clockwise winding structures (shown in Figure 3), where thread separation releases tension stress. This makes it less energetically demanding for DNA double-strand to separate.[17,19]

Positive supercoiling is left-handed rotation tangling DNA duplex into clockwise winding structures (Figure 3).[17] This kind of supercoil develops the unrolling of DNA from histones. This type of tension is also a necessary factor in changing the conformation of the thread, so RNA polymerase can effectively elongate. In thermophiles, the positive supercoil protects DNA from thermal denaturation.[19,20]

Catenanes (linked circular molecules that appear at the end of replication of circular DNA)[21] and knots are examples of other topological problems that are resolved by topoisomerases.[22]

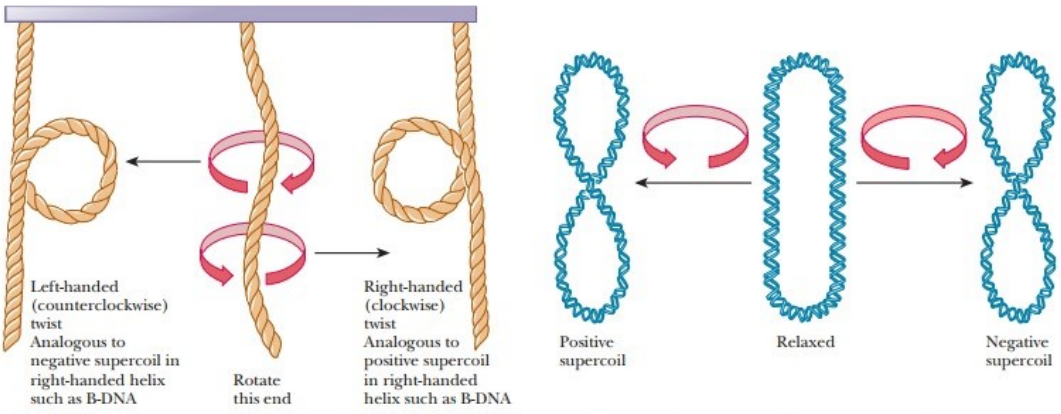

Figure 3 Supercoiled DNA topology. If the strand starts winding to the right, the strand becomes overwound. If the strand starts rotating to the left, the strands become underwound and begin to separate. On the left is stranded DNA, and on the right is circular. Taken from https://www.brainkart.com/article/How-does-prokaryotic-DNA-supercoil-into-its-tertiary-structure-_27536/ [17]

Without topoisomerases, DNA supercoils would be permanently tangled, and become unreadable. This would be fatal for the cell. Topoisomerases are enzymes located in the nucleus and mitochondria[22] occurring in all forms of life - eukaryotes, bacteria, and archaea.[23] Their main mission is to control the topological state of DNA by single or double-stranded cleavage of DNA molecules. In bacteria, but not in eukaryotes, can be found type of topoisomerase (called gyrase) able to form negative supercoil.[24]

Human topoisomerases are sorted into two general types: type I and type II. These types are further divided into subtypes. Human cells contain 6 of these subtypes – TOP1 and mitochondrial TOP1 (type IB), TOP2A and TOP2B (type IIA), and TOP3A with TOP3B (type IA). Each of these enzymes has its purpose and mechanism of action. Mechanisms of action are indicated in Figure 4.[22]

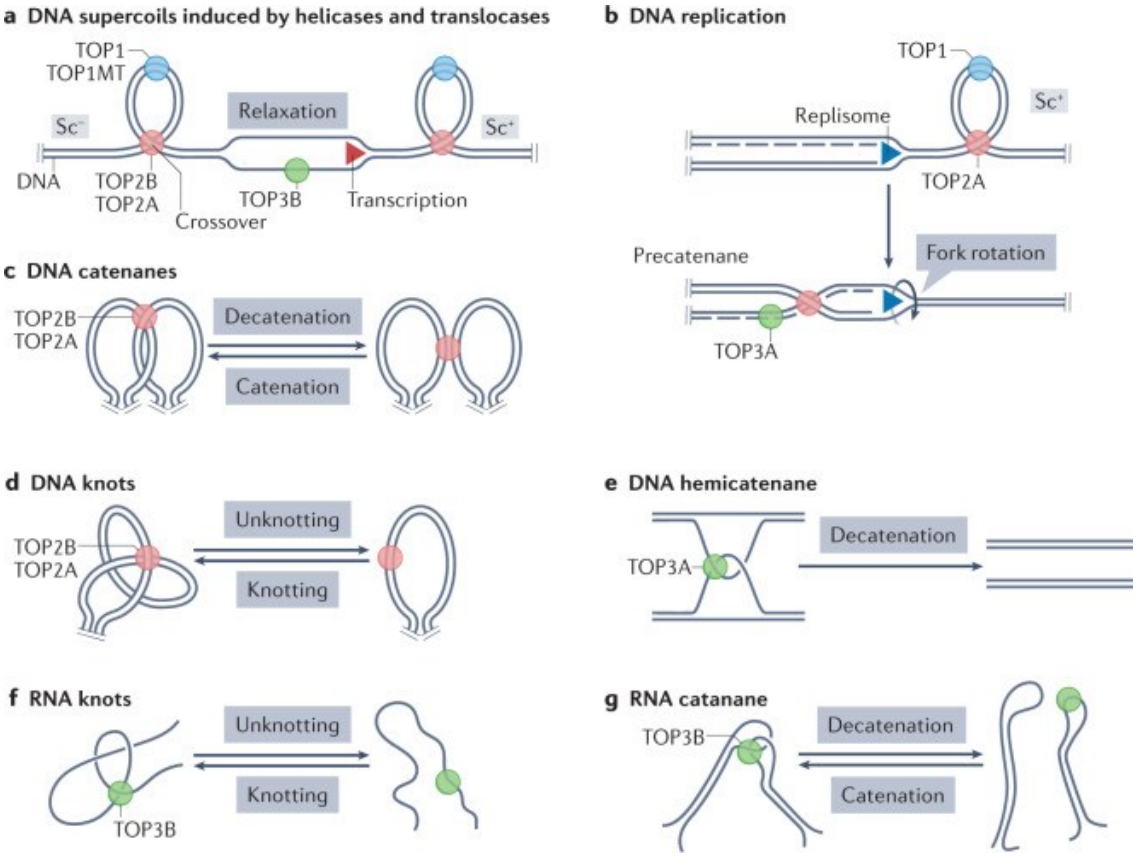

*Figure 4 Actions of topoisomerases. **A**-opening DNA duplex generates positive supercoiling (Sc+) in front of and negative supercoiling (Sc-) behind transcription enzymes."**B**-replication forks generate Sc+ in front of the replicating replisome. If the replisome swivels due to the twisting force, Sc+ diffuses behind the replisome and generates precatenanes, which are removed by Top2A. Top3A may also remove precatenanes if they include single-stranded DNA segments"(taken from Pommier et al.)*[22]*. **C** – decatenation of DNA by double-strand passage (molecule of DNA is passed through the double-strand break) **D** – knots removed by double-strand passage **E** – single-strand passage (passing a single thread of DNA through break made in another DNA thread) **F** – single-strand passage of intramolecular RNA knots (made by only RNA topoisomerase Top3B). **G** – single-strand passage of RNA catenanes. Taken from Pommier et al.*[22]

2.3.1 Topoisomerase I

Topoisomerases I break one strand of DNA, transit a thread of DNA through, and then reseal it. More precisely, they form transient phosphotyrosine covalently bond with the 5′ or 3′ end of the broken DNA strand. This is powered by torsional stress in the supercoiled DNA. Except for DNA-gyrase, these enzymes don´t need any high-energy cofactor for function. They are divided into two main subclasses – IA and IB.[16,25,26]

Subclass IA forms a phosphotyrosine bond at the 5′ end of the DNA strand. It requires bivalent cations and single-stranded regions of DNA. This subclass relaxes only negatively supercoiled DNA. Human cells contain topoisomerase III α and β while bacterial cells contain topoisomerase I and III.[16,25,26]

Subclass IB attaches tyrosine from its active site to the 3′ end of the broken DNA strand. This group of enzymes doesn´t need bivalent ions and can relax negatively and also positively supercoiled DNA. This makes it distinct from the other types of topoisomerases. Human cells contain topoisomerase I while bacterial cells contain topoisomerase IB.

Topoisomerases I, especially eucaryotic subclass IB, are targets of anticancer drugs.[16,25,26]

2.3.2 Topoisomerase II

The mechanism of action of Topoisomerase II is creating a transient double-stranded break in the DNA thread. Eukaryotic TopoII are large magnesium ions and ATP-dependent enzymes with homodimer structure. The energy of ATP hydrolysis is needed for conformational changes of the enzyme, and it is not directly involved in DNA cleavage.

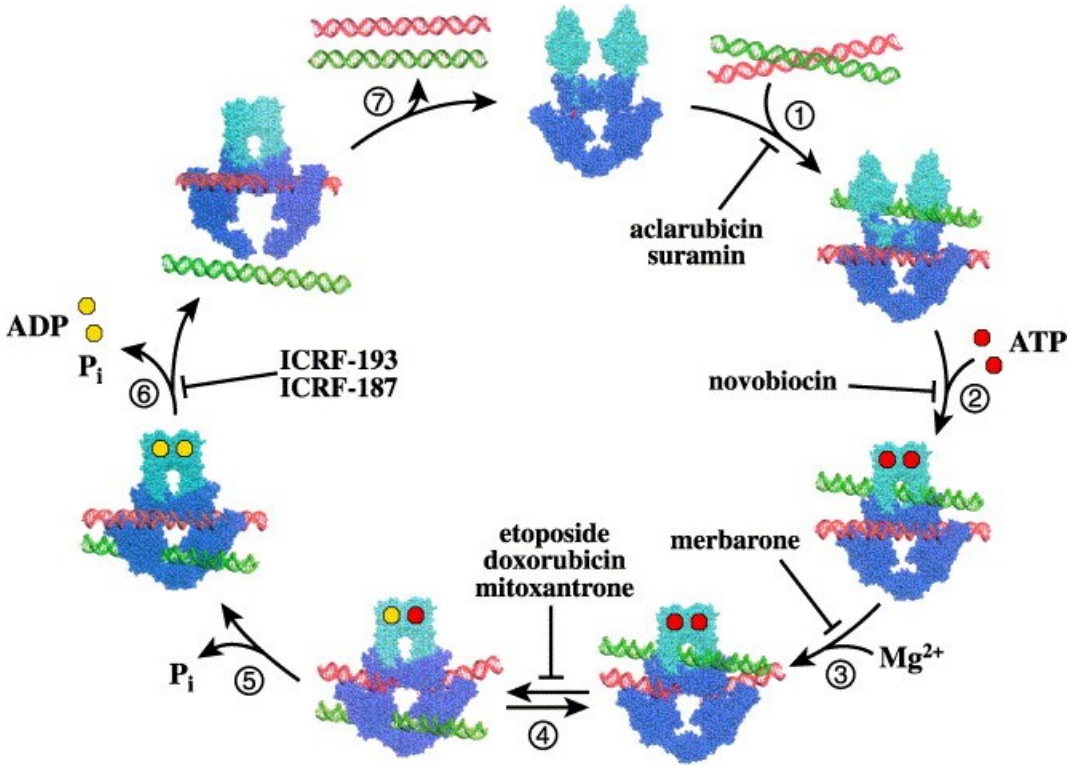

Figure 5 The catalytic cycle of TopoII. The catalytic cycle starts when the enzyme binds two double-stranded DNA segments - red G-segment (G =„gated“) and green T-segment (T =transported) (1st step). In the second step, ATP molecules bind into ATPase domains leading to dimerization of these domains (2nd step) followed by Mg2+ dependent cleavage of the G-segment (3rd step). Next, ATP hydrolysis facilitates the transport of the T-segment through the split G-segment (4th step). The G-segment is then resealed and the remaining ATP is hydrolyzed (5th step). In the end, ADP molecules are discharged, and the DNA segments are released one by one (6th and 7th step).[27–29] *Taken from Larsen et al.*[28]

TopoII forms phosphotyrosine linkage with two tyrosines located in the active site of the enzyme and a pair of 5´-phosphates. This ensures that the DNA strand can be resealed after cleavage. Detailed mechanism of action is described in Figure 5.[27]

Vertebrates carry two isoforms of TopoII – Topoisomerase II α and β.[30] α isoform is active during replication, specifically during mitosis and anaphase. High concentration of this isoform has been reported in highly proliferating cells, such as malignant cells. β isoform, on the other hand, shows activity in all post-mitotic cells independently of the cell cycle. It was proved, that β isoform has a similar function as isoform α *in vitro*. However, the *in vivo* function of β isoform seems inessential for proliferating cells and thus its function *in vivo* remains unclear.[31] It is presumed that this isoform is performing „housekeeping" actions in the post-mitotic phase like repairing DNA and enabling transcription. It is assumed that inhibition of this isoform is responsible for severe side effects, like secondary malignities or cardiotoxicity, of current anticancer therapy targeting topoisomerase II.[32] Increasing the selectivity of TopoII inhibitors to α isoform could be the right way in the development of effective anticancer drugs.

2.4 Inhibitors of DNA topoisomerases

2.4.1 Inhibitors of Topoisomerase I

Inhibitors of hTopoI are divided into two big groups – camptothecin inhibitors and non-camptothecin inhibitors.[33]

The first developed drug targeting TopoI was natural alkaloid 20(*S*)-camptothecin (shown in Figure 6) isolated from the bark of *Campthotheca acuminata*.[34] Substances belonging to the group of camptothecin inhibitors trap DNA cleavage complex. Turning temporary complex into persistent cytotoxic adducts leads to excessive DNA damage and cell death – this mechanism of action is classified as TopoI poisoning.[35]

The downsides of camptothecin treatment are bad solubility, instability, unpredictable drug-drug interactions, and severe side effects like leukopenia and diarrhoea. Therefore, semi-synthetic derivates with better properties are being developed. Several derivates with improved water solubility are already registered - irinotecan for colon cancer, topotecan for ovarian cancer, and belotecan for ovarian and small lung cancer (shown in Figure 7). More derivatives are in clinical trials.[33–35]

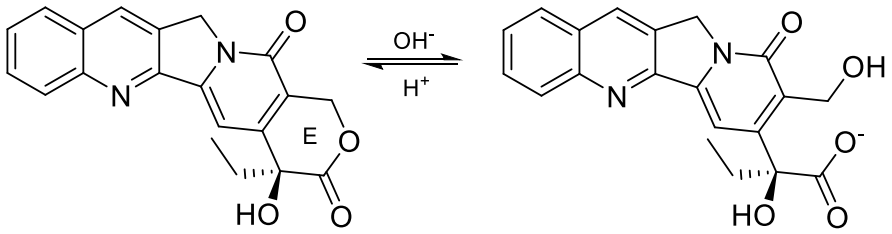

Figure 6 Chemical structure of camptothecin. Lactone E-ring is unstable in physiological pH and converts into carboxylate. The carboxylate form is inactive and binds to serum albumin. Taken from Li et al.[36]

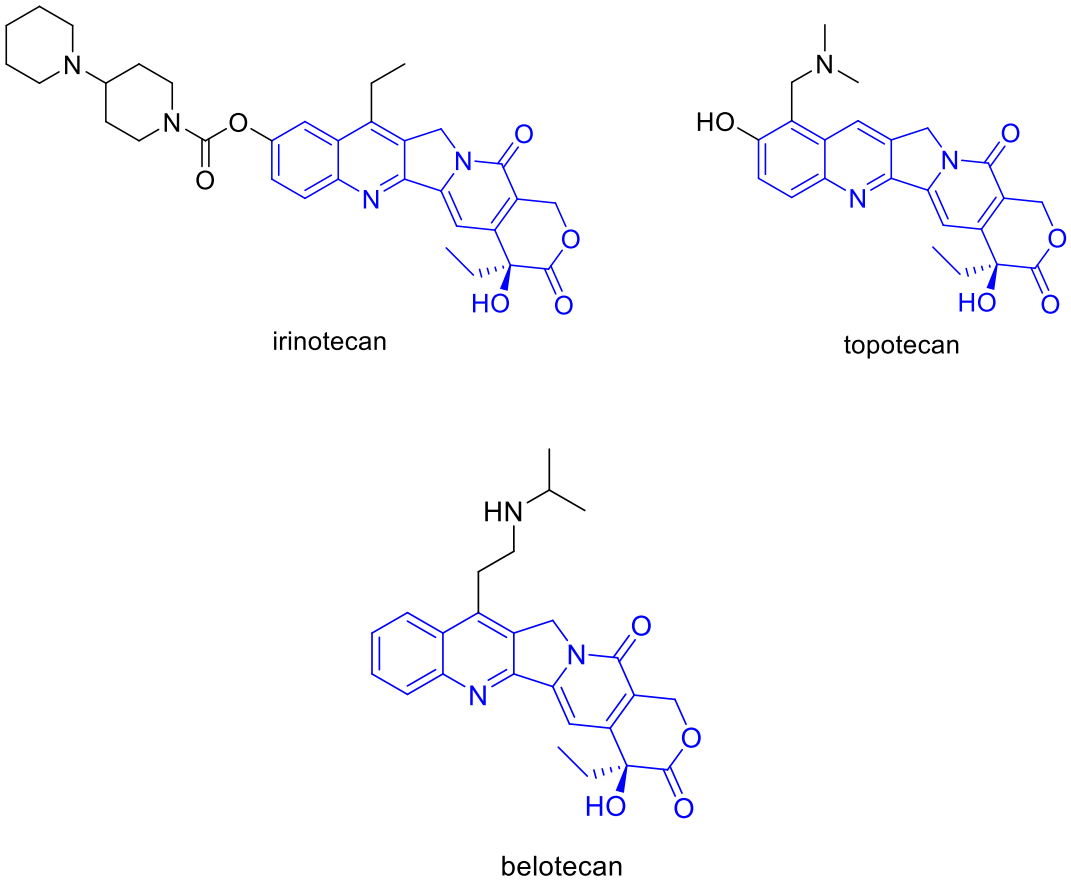

Figure 7 Chemical structures of irinotecan, topotecan and belotecan with highlighted camptothecin molecule.

The issue of bad stability led to another group of compounds – non-captothecin inhibitors. Among the most important scaffolds used in this group belong indolocarbazole (e.g. becatecarin and edotecarin are in clinical trials), indenoisoquinoline (e.g. indimitecan, indotecan and LMP744 are in clinical development) and dibenzonaphthyridinone (possessing great cytotoxicity).[34,35]

2.4.2 Inhibitors of Topoisomerase II

Current inhibitors of hTopoII act as non-specific agents inhibiting both α and β isoforms without difference.[37] As mentioned earlier, inhibition of isoform β is probably responsible for severe side effects.[32] The development of novel anticancer compounds focuses on inhibitors selective to α isoform. Inhibitors of hTopoII are divided into two big groups: poisons and catalytic inhibitors.[31]

2.4.2.1 TopoII poisons

TopoII poisons were discovered in the 1960s.[31] Mechanism of action is creating covalent complexes with DNA (Figure 5 step 4) leading to DNA damage and, in most cases, induction of cell apoptosis. In rare cases, the use of these drugs can lead to chromosome translocation triggering secondary malignities (there are documented cases of leukaemias caused by such translocation).[38] Another severe side effect is cardiotoxicity. The previous presumption was that the cardiotoxicity of substances like doxorubicin (Figure 8) is the result of the creation of free oxygen radicals damaging cell membranes, but it was disproved. It was discovered that β isoform is highly expressed in cardiomyocytes and its inhibition by poisons takes away the "housekeeping" function of the cell as well as creates a damaging complex. This leads to excessive damage to the heart. Despite these severe side effects, hTopoII poisons such as daunorubicin, doxorubicin, etoposide (Figure 8), and mitoxantrone (Figure 9) are widely used in clinical practice.[32,37]

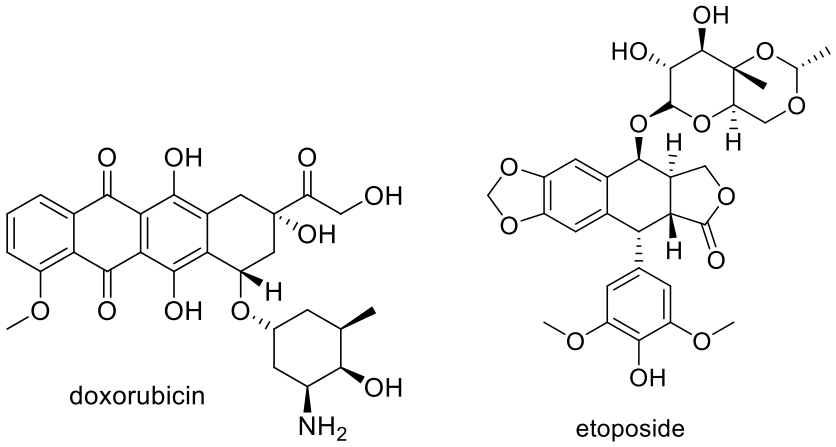

Figure 8 Chemical structures of doxorubicin and etoposide.

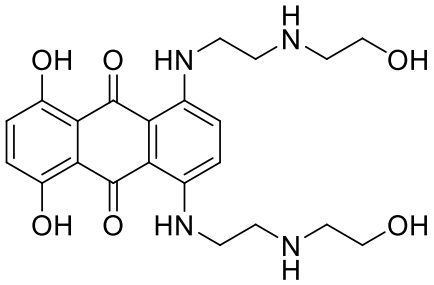

Figure 9 Chemical structure of mitoxantrone.

2.4.2.2 Catalytic inhibitors

Catalytic inhibitors, in contrast with poisons, do not create a covalent cleavage complex between hTopoII and DNA, and therefore they cause just minimal damage to the DNA. They act through various mechanisms e.g. blocking hTopoII binding to DNA (Figure 3, step 1; e.g. aclarubicin – can be seen in Figure 10), inhibition of ATP-binding site of hTopoII (Figure 3, step 2; e.g. novobiocin – can be seen in Figure 10), preventing the formation of hTopoII-DNA complex (Figure 3, step 3; e.g. merbarone – can be seen in Figure 10) or inhibition of ATP hydrolysis making it impossible for the enzyme cleaves the DNA (Figure 3, step 6; dexrazoxane – can be seen in Figure 10). This results in effective inhibition of hTopoII activity with low genotoxicity.[39,40] Dexrazoxane is the only molecule approved for clinical use, however, it is used just to prevent cardiotoxicity of anthracycline drugs (depletion of hTopoIIβ → anthracycline cannot bind and create DNA damaging complex).[41]

The most promising group of catalytic inhibitors are considered ATP-competitive inhibitors. Compounds in this group vary in basic heterocyclic scaffolds including for example purine and pyridine analogues, thiosemicarbazones, and nitrofurans. *N*-Phenylpyrrolamides are a novel chemotype of ATP-competitive inhibitors discovered at the Faculty of Pharmacy at the University of Ljubljana through screening of previously prepared bacterial topoisomerase inhibitors. Newly prepared compounds described in this thesis are presumed to have the ability to bind into the ATP-binding site of hTopoIIα.[31,40,42]

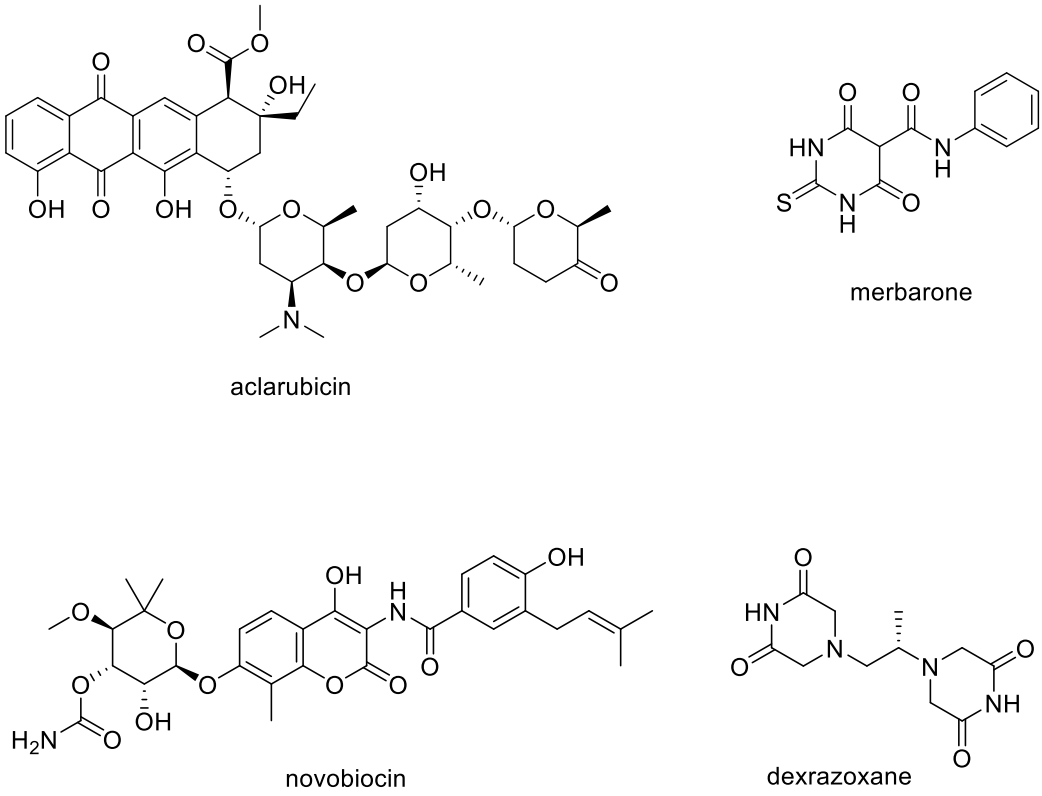

Figure 10 Chemical structures of aclarubicin, merbarone, novobiocin and dexrazoxane.

2.5 Structure-activity relationship

A novel chemotype of ATP-competitive inhibitors, *N*-Phenylpyrrolamides, was discovered during the screening of an in-house library of ATP-competitive inhibitors of bacterial DNA gyrase and topoisomerase IV.[31] The in-house library of Skok et al. was based on oroidin and kibdelomycin, natural products with antibacterial activity. Both compounds have dihalogen-substituted pyrrolamide moiety (shown in Figure 11), which was assumed to be crucial for binding into the ATP-binding site, and both are inhibitors of bacterial gyrase B and topoisomerase IV.[43,44] Screening provided 20 hits whose structure was explored, and 13 compounds were synthesized to better understand the new structural type of hTopoII ATP-competitive inhibitors.[31]

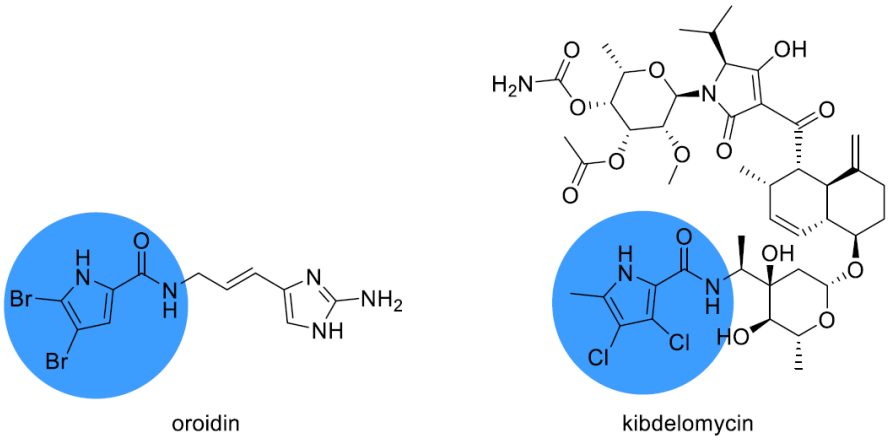

Figure 11 Chemical structures of natural compound oroidin and kibdelomycin with highlighted pyrrolamide moieties. *Taken from Skok et al.*[31]

A template for further design modifications was developed (also represents the smallest binding motive into the ATP-binding cavity; Figure 12). Interactions in the binding cavity are shown in Figure 12.[45]

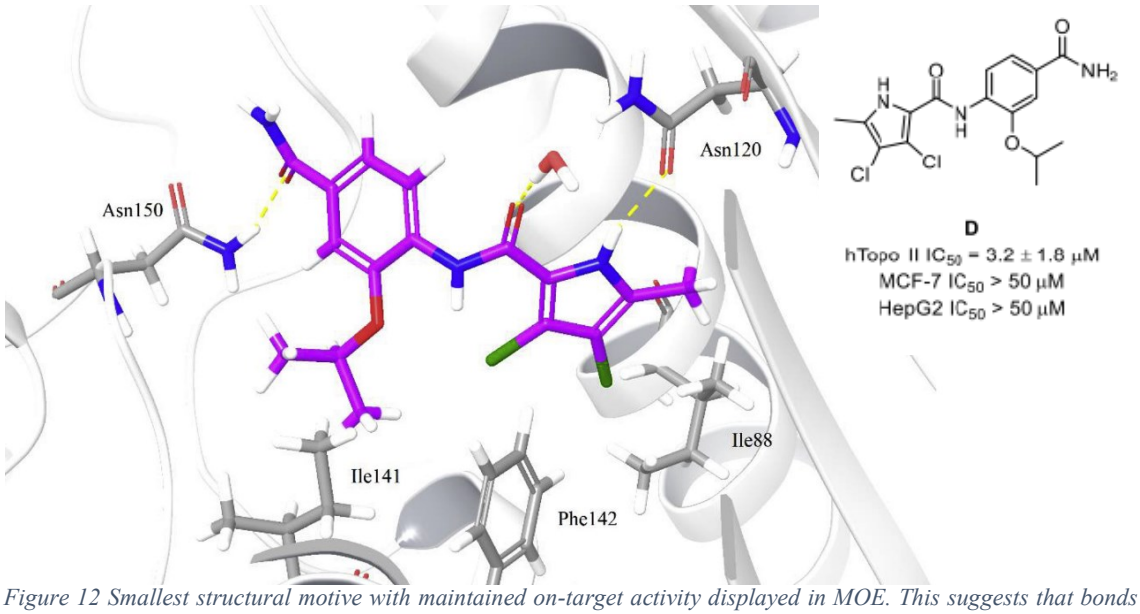

Figure 12 Smallest structural motive with maintained on-target activity displayed in MOE. This suggests that bonds with asparagine 120 and crystallographic water are crucial for the activity. Later was discovered that a bond with this asparagine is preferable but not necessary. Taken from Skok et al.[45]

The follow-up research confirmed that dihalogen-substituted pyrrolamide moiety is essential for on-target activity. According to docking results, 3,4-dichloro-5-methyl moiety fits better in the hydrophobic pocket of the adenine binding site than compounds with 4,5-dibromo pyrrole, which resulted in better on-target activities of first mentioned group of compounds. As mentioned in Figure 12, pyrrole carboxamide moiety forms hydrogen bonds with Asn120 and crystallographic water. The hydrogen bond between

Asn150 and the primary carboxamide group in position four is beneficial for the activity, but not necessary. The inhibitory activity can be preserved by the optimal selection of substituent in position two of the benzene ring. Benzene ring manifested as a functional central scaffold with substituents in positions two and four or two and five. This binding mode makes *N*-Phenylpyrrolamides unique because they occupy different binding pockets compared to current inhibitors. The amide group in position four is advantageous for the on-target activity. However, it is associated with lowering the cytotoxicity of synthesized compounds on whole cells. Deletion of this group resulted in increased cytotoxic effects, probably because of lower polar surface area and therefore better passive diffusion of the compounds into the cells. It can be observed for example in the latest study of Skok et al. where the best on-target activity was obtained by compound 47d (Figure 13) with carboxamide in position four and basic centre attached to benzyloxy substituent connected in position two. However, the best cytotoxicity was achieved by compound 53b (Figure 13) without carboxamide.[45]

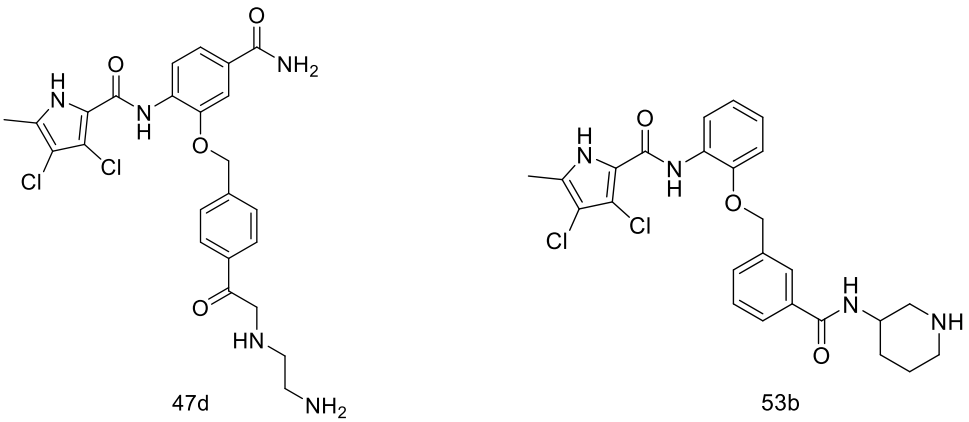

Figure 13 Compounds 47d and 53b. Compound 47d was the most on-target potent compound of the previous study (IC50 hTopoII = 0.67 μM). Compound 53b was the most cytotoxic compound of the previous study (IC50 MCF-7/HepG2 = 140 nM/ 130 nM; IC50 hTopoII = 7.7 μM). Taken from Skok et al.[45]

It was further found that the substituent in position two should be ideally *para*-substituted or *meta*-substituted by benzyloxy fragment with the basic group. Extension and free rotation of the benzyloxy fragment allow the compound to reach and interact with amino acid residues in the phosphate-binding area of the ATP-binding site.[45] For better orientation, the structure-activity relationship is illustrated in Figure 14.

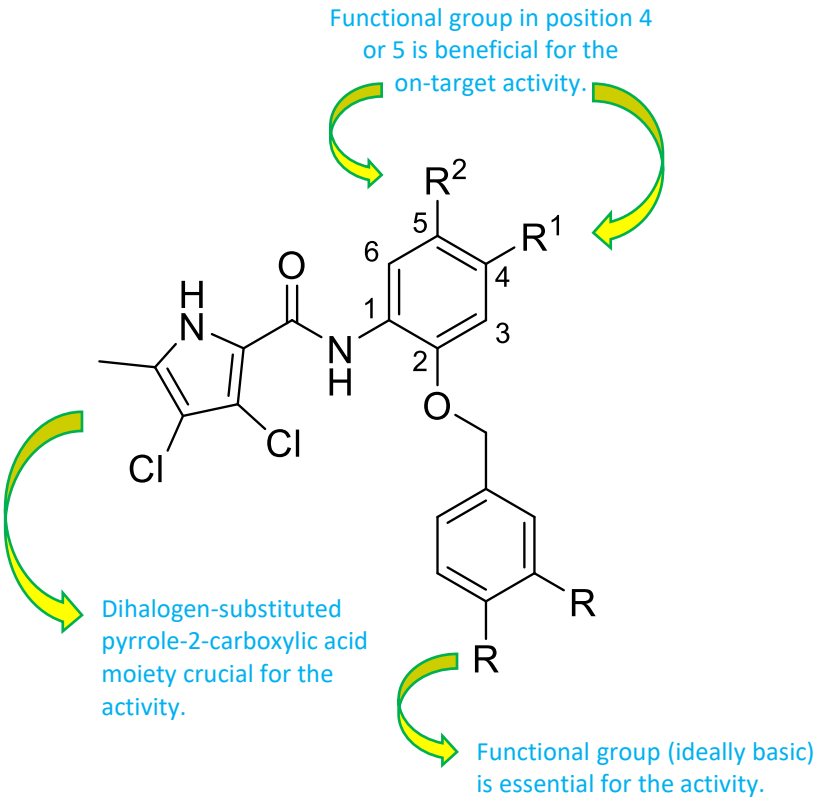

Figure 14 Structure-activity relationship of the most potent N-Phenylpyrrolamides from the latest study.

3. Experimental part

3.1 Synthesis of IMD 0 series - Complete reaction scheme

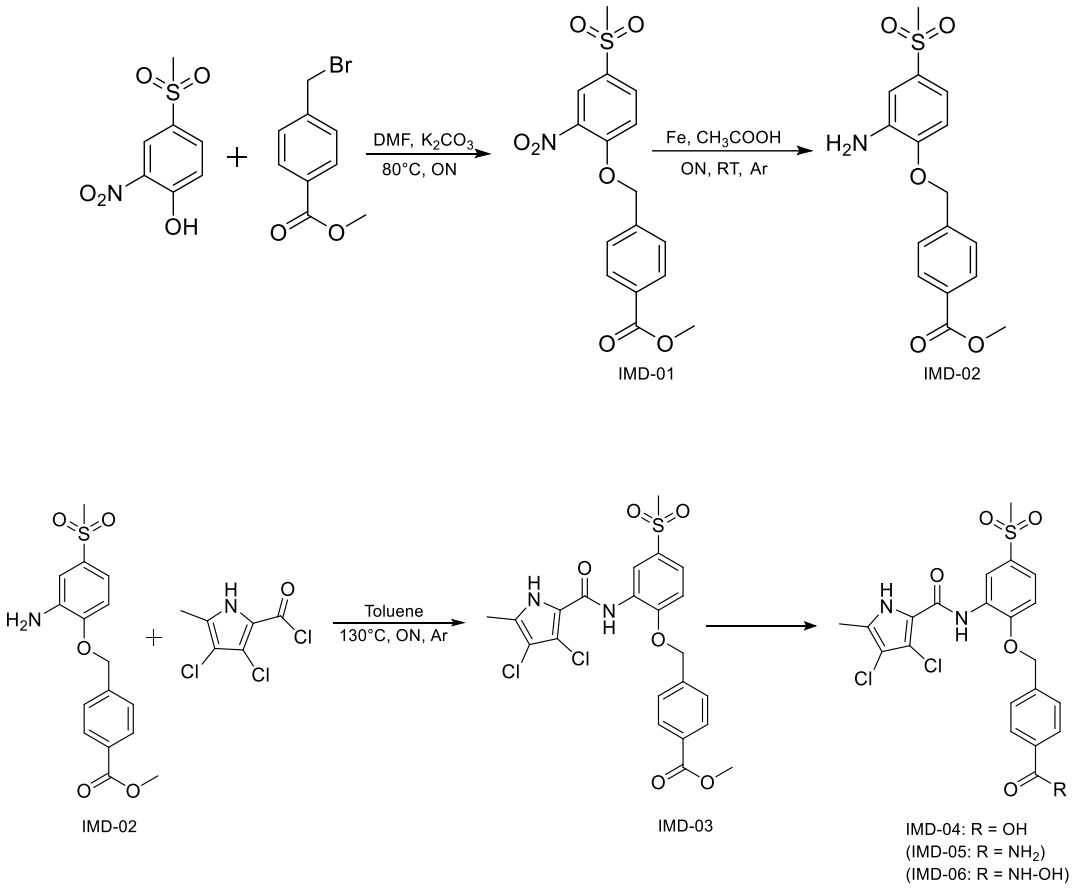

3.1.1 Synthesis of IMD-01

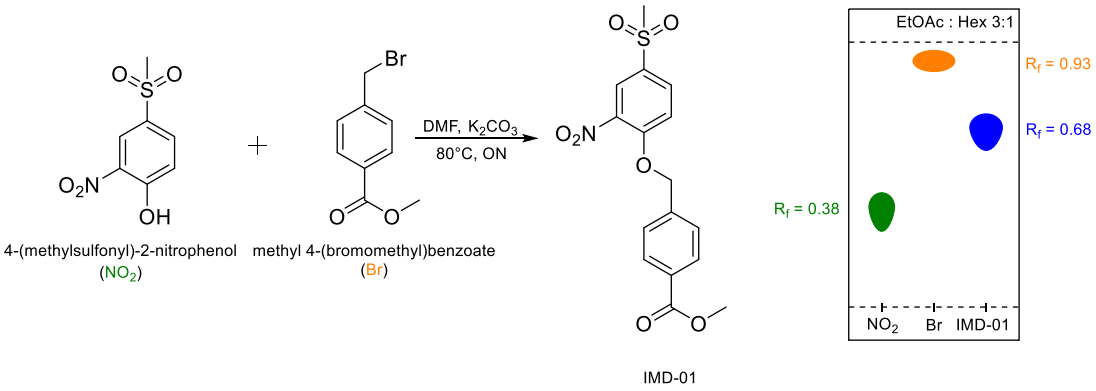

Reagents	**m(mg)/V(ml)**	**n (mmol)**	**MW (g/mol)**	**Equivalents**
Nitrophenol	437 mg	2.0	217.20	1.0
Alkylhalogenide	457 mg	2.0	229.07	1.0
K_2CO_3	553 mg	4.0	138.21	2.0
DMF	5.0 ml		73.09	

4-(methylsulfonyl)-2-nitrophenol (2 mmol) was dissolved in 5ml of anhydrous DMF. K_2CO_3 (4 mmol) and methyl 4-(bromomethyl)benzoate (2 mmol) were added and the reaction mixture was stirred overnight at 80° C.

After that, K_2CO_3 was neutralized with 8 ml of 1M HCl. Then the reaction mixture was washed with distilled water and a precipitate occurred. Precipitate was filtered and washed with distilled water. The yield was 501 mg (68%). Results of the HPLC-MS showed one major peak 94.5% pure. Therefore, it was considered a satisfying result, and it was proceeded on.

3.1.2 Synthesis of IMD-02

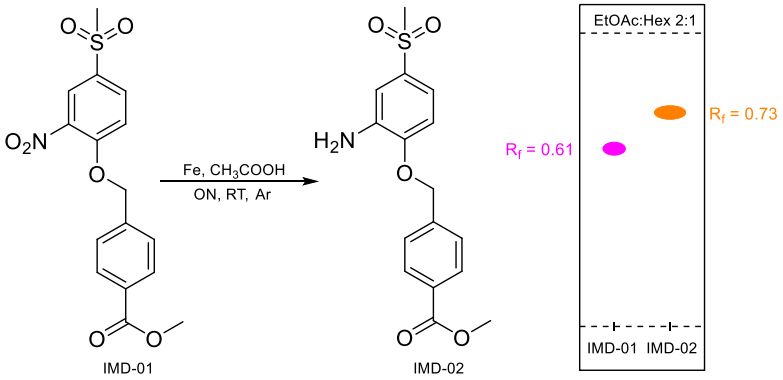

Reagents	**m(mg)/V(ml)**	**n (mmol)**	**MW (g/mol)**	**Equivalents**
IMD – 01	491 mg	1.3	367.00	1.0
Fe	753 mg	13.5	55.85	10.4
CH_3COOH	13.0 ml		60.05	

IMD-1 (1.3 mmol) was suspended in 13 ml of neat CH_3COOH, and Fe (13.5 mmol) was added. The reaction mixture was stirred at room temperature overnight under an argon atmosphere. The reaction was incomplete, so 5 more equivalents of iron were added (372 mg), and the reaction mixture was stirred under argon another night.

After that, the crude reaction mixture was neutralized with NH_3 solution in water (25% m/m), transferred to a separating funnel, and extracted with ethyl acetate (200 ml). Due to the presence of iron, a hardly separable mixture of phases was formed. The water phase was separated and divided into two beakers due to its volume. The content of both beakers was extracted with ethyl acetate (100 ml). Organic phases were combined and washed with 50 ml of brine, dried over anhydrous Na_2SO_4, and evaporated under reduced pressure. The purity showed by HPLC-MS was 100%. The yield of this reaction was 433 mg (96%).

3.1.3 Synthesis of IMD-03

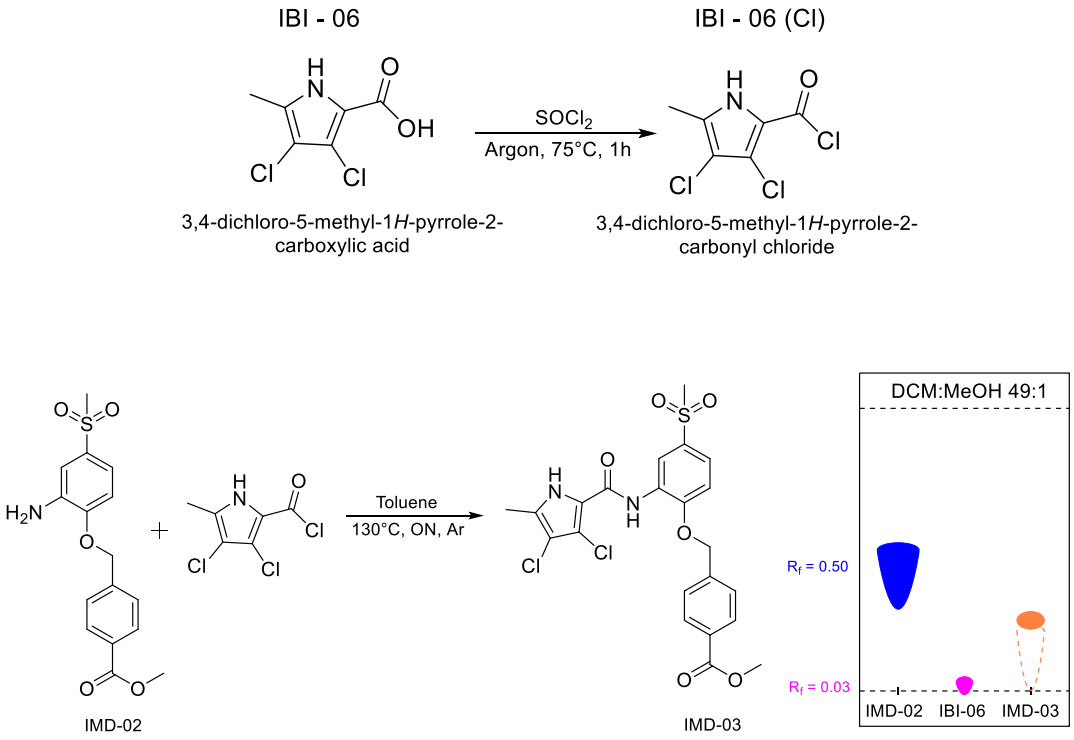

Reagents	m(mg)/V(ml)	n (mmol)	MW (g/mol)	Equivalents
IBI - 06	103 mg	0.5	194.01	1.3
$SOCl_2$	1.0 ml		118.97	
IMD - 02	147 mg	0.4	335.08	1.0
Solvent	5.0 ml			

Compound IBI-06 was synthesized and provided by Professor Ilaš´s group. IBI-06 (0.5 mmol) was stirred in excess of $SOCl_2$ at 75° C for 1h under an argon atmosphere. $SOCl_2$ was evaporated after that using a water pump and then dried for 10 minutes under reduced pressure. This intermediate for the following step, IBI-06(Cl), was very sensitive to air moisture.

IMD-02 (0.4 mmol) and anhydrous DCM were carefully added to IBI-06(Cl), and the reaction mixture was stirred overnight at room temperature under an argon atmosphere. This process was unsuccessful, so the reaction conditions were adjusted. DCM was replaced by anhydrous toluene and reaction temperature was increased to 130° C under a condenser.

Purification was done by filtration. Precipitate was washed with a variety of solvents and 125 mg (56%) of the pure compound was obtained.

Attempts of TLC were unsuccessful due to the bad solubility of precipitate in any conventional solvent. Therefore, preparation of the sample for HPLC-MS was very difficult as well. At first, just small peaks with small absorption appeared (Figure 15).

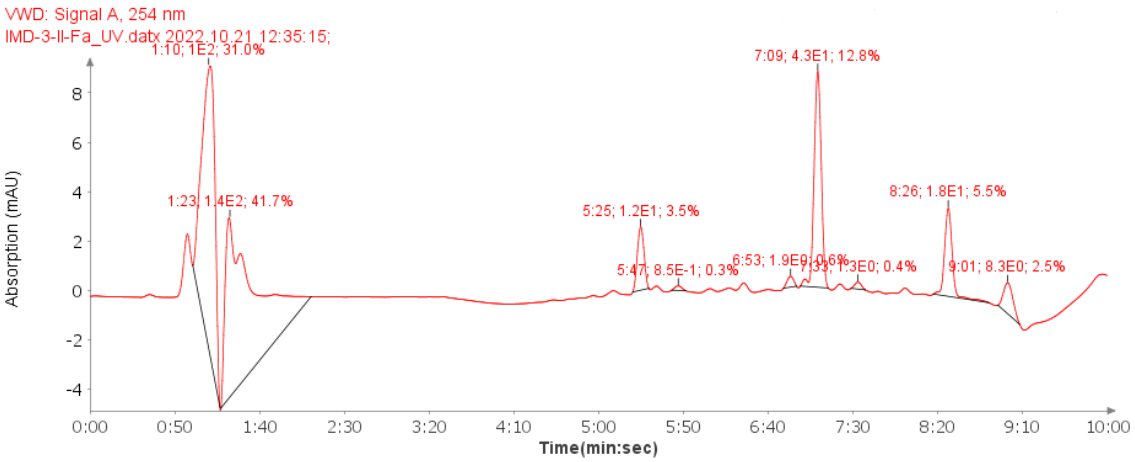

Figure 15 HPLC of IMD-03 before adjusting the sample preparation.

Another approach for the preparation of the HPLC-MS sample was used. Instead of adding DMSO into the MeOH mixture with the compound, the compound was dissolved in 100 µl of DMSO. 10 µl of this solution were diluted in 1 ml of 60% ACN and 40% water solution of 0.1% TFA, but it precipitated out. Heating and ultrasound did not improve the solubility of the substance. Another preparation with half of the sample concentration (5 µl) was successful. A nice clear peak of 97.3% purity (Figure 16) appeared on the chromatogram. It was considered clear enough to continue with reactions.

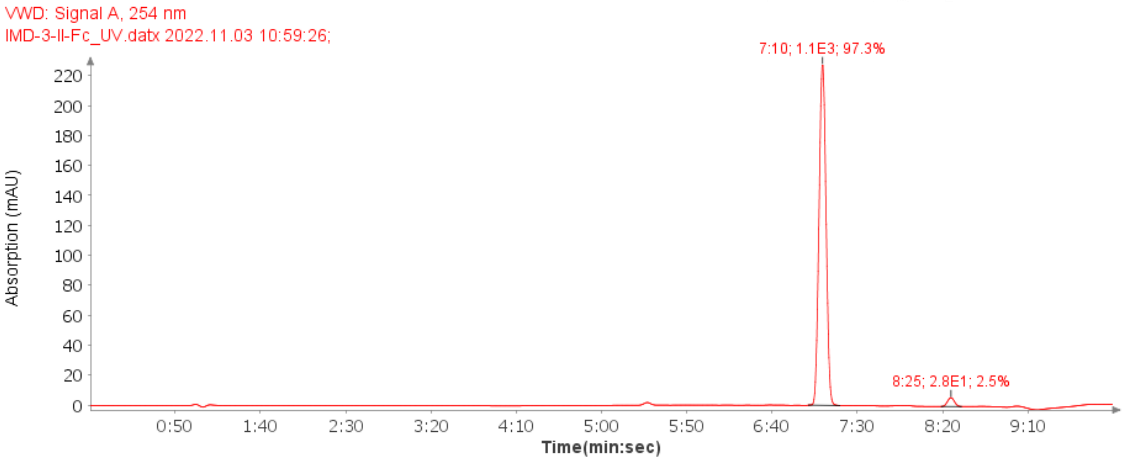

Figure 16 HPLC of IMD-03 after adjusting the sample preparation.

3.1.4 Synthesis of IMD-04

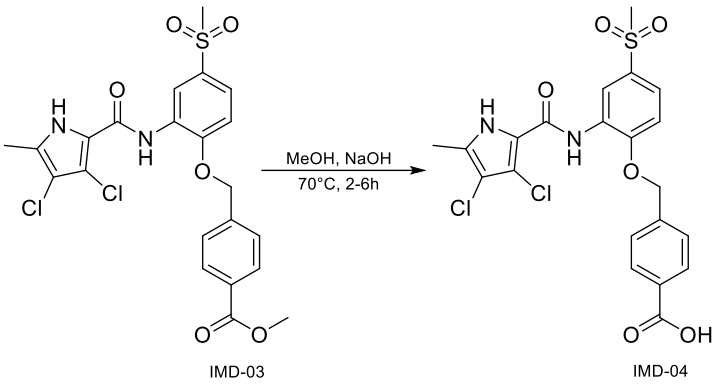

Reagents	m(mg)/V(ml)	n (mmol)	MW (g/mol)	Equivalents
IMD - 03	42 mg	0.1	335.08	1.0
NaOH	40 mg	1.0	40.00	10.0
MeOH	0.4 ml		32.04	

IMD-03 was supposed to be used for the synthesis of carboxylic acid, hydroxamic acid, and amide. 1/3 of the product (42 mg = 0.1 mmol) was suspended in anhydrous MeOH, 1M NaOH (1 mmol) was added, and the reaction mixture was stirred overnight at room temperature. The first attempt of the reaction was unsuccessful, but 13 mg of the starting material (IMD-03) was regenerated as a pale compound. The reaction was repeated using the same procedure as before. The second attempt of the hydrolysis ran for 2 days when 5 more equivalents of fresh 1M NaOH solution were added to the reaction. The reaction was heated after another day to 70° C for 2–6 hours. When the reaction was finished (HPLC-MS showed no IMD-03), the reaction mixture was acidified with 1M HCl to pH 2. The precipitate was filtered and washed with distilled water. The yield of the hydrolysis was 21 mg (58%) and purity according to HPLC-MS was 97.6%.

3.2 Synthesis of IMD 1 series – complete reaction scheme

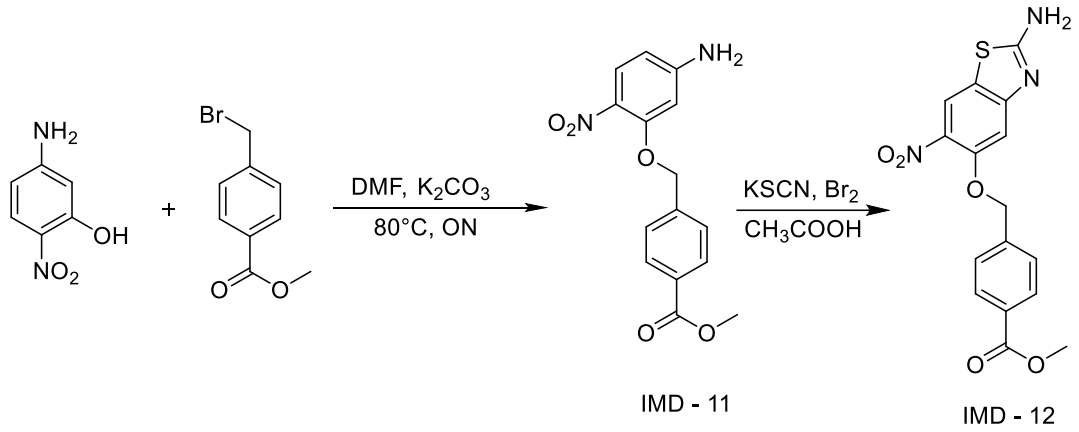

IMD - 11

IMD - 12

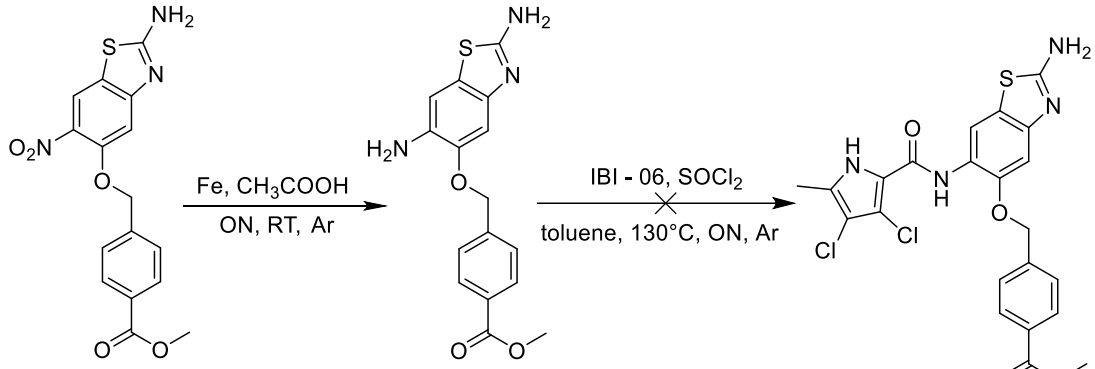

IMD - 12

IMD - 13

IMD - 14

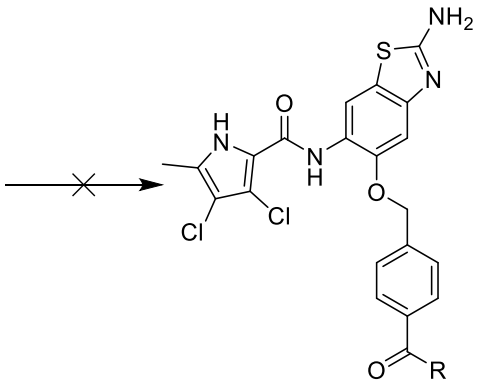

IMD-15 : R = -OH
IMD-16 : R = -NH_2
IMD-17 : R = -NH-OH

3.2.1 Synthesis of IMD-11

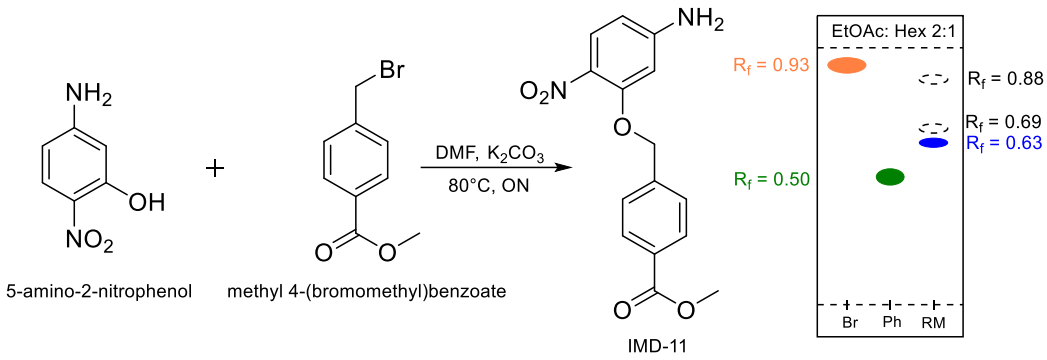

Reagents	m(mg)/V(ml)	n (mmol)	MW (g/mol)	Equivalents
Nitrophenol	321 mg	2.1	154.13	1.0
Alkylhalogenide	468 mg	2.1	229.07	1.0
K_2CO_3	589 mg	4.3	138.21	2.0
DMF	5.0 ml		73.09	

5-amino-2-nitrophenol (2.1 mmol) was dissolved in 5 ml of anhydrous DMF. K_2CO_3 (4.3 mmol) and methyl 4-(bromomethyl)benzoate (2.1 mmol) were added and the solution was stirred overnight at 80° C.

K_2CO_3 was then neutralized with 8.5 ml of 1M HCl and the reaction mixture was washed with distilled water. Precipitate occurred. After filtration and analysis of precipitate, the dry loading approach of column chromatography was done with mobile phase EtOAc:Hex 1:1 (Figure 17). The yield after column chromatography was 330 mg (53%). The sufficient purity was confirmed by HPLC-MS (96 %).

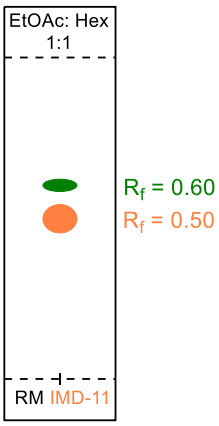

Figure 17 TLC of the reaction mixture of IMD-11 before column chromatography. The orange spot is IMD-11, green spot is impurity.

3.2.2 Synthesis of IMD-12

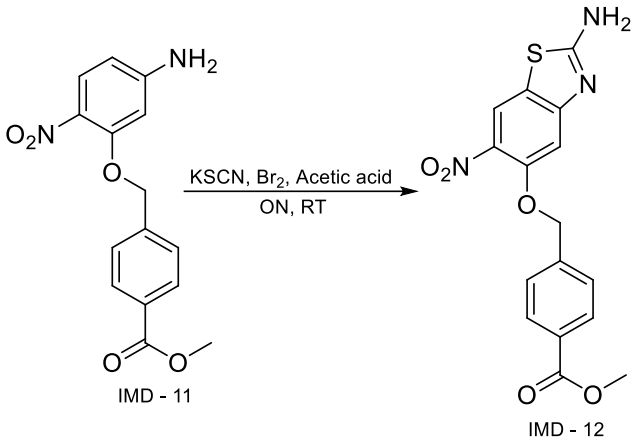

Reagents	**m(mg)/V(ml)**	**n (mmol)**	**Mw (g/mol)**	**Equivalents**
IMD - 11	302 mg	1.0	302.10	1.0
KSCN	390 mg	4.0	97.18	4.0
Br_2	103 µl	2.0	79.90	2.0
CH_3COOH	14.0 ml		60.05	

IMD-11 (1 mmol) was dissolved in neat acetic acid and stirred for 10 minutes. KSCN (4 mmol) was added and the reaction mixture was stirred until complete dissolution. After that, the mixture was cooled down to 0° C in an ice bath and Br_2 (2 mmol) in 1 ml of neat acetic acid was added dropwise. The reaction mixture was stirred at room temperature overnight. Precipitate occurred. The reaction was filtered and washed with a variety of solvents.

The precipitate was insoluble in any conventional solvent and even in boiling DMSO. Nevertheless, HPLC-MS, TLCs, and NMR were done. On TLC, the coloured spot assigned to the product stayed at the start. The chromatogram showed only small peaks. NMR showed that it is probably the desired compound but was inconclusive due to the intensity of signals. Another step of synthesis was done with all of the compound (129 mg = 36% yield) anyway.

3.2.3 Synthesis of IMD-13

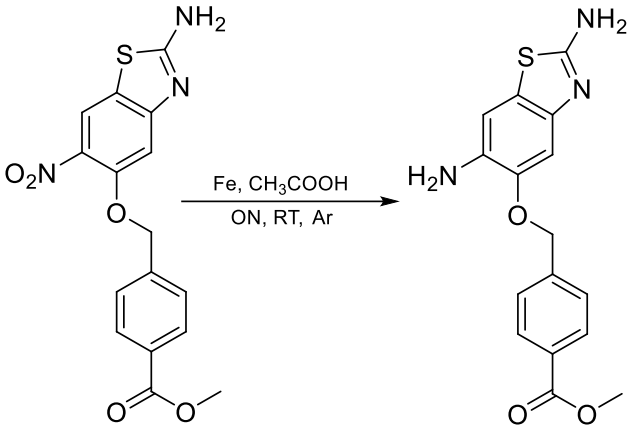

Reagents	**m(mg)/V(ml)**	**n (mmol)**	**MW (g/mol)**	**Equivalents**
IMD - 12	116 mg	0.3	359.10	1.0
Fe	191 mg	3.4	58.85	11.3
CH_3COOH	6.0 ml		60.05	

IMD-12 (0.3 mmol) was suspended in neat acetic acid, and Fe (3.4 mmol) was added. The reaction mixture was stirred overnight at room temperature under an argon atmosphere. The mixture was neutralized with NH_3 solution in water (25% m/m). Even though that solubility was slightly improved, the attempt of separation into EtOAc failed. The mixture was boiled in EtOAc to improve solubility but without any effect. Therefore, this series of reactions was abandoned.

3.3 Synthesis of IMD 2 series – complete reaction scheme of starting material

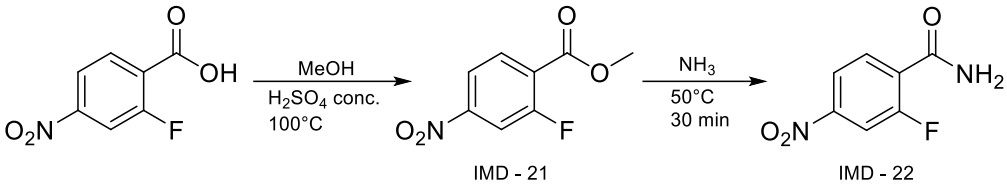

3.3.1 Synthesis of IMD-21

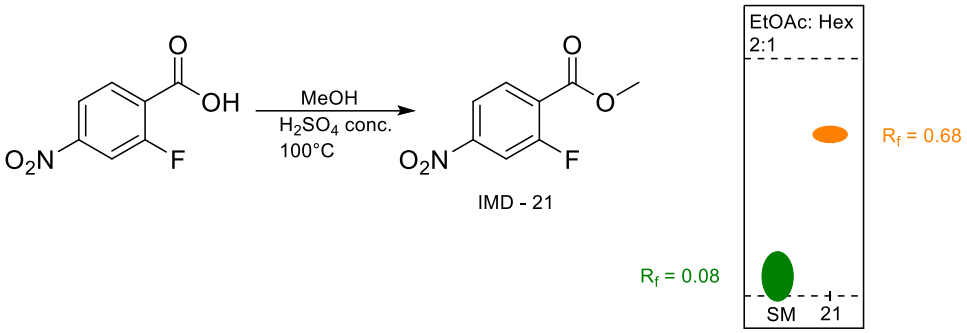

Reagents	m(mg)/V(ml)	N(mmol)	MM(g/mol)	Equivalents
Nitrobenzoic ac.	5 g	27.3	185.11	1.0
MeOH	54.5 ml		32.04	
H_2SO_4	5.5 ml	0.2 ml/mmol	98.08	

2-fluoro-4-nitrobenzoic acid (27.3 mmol) was dissolved in anhydrous MeOH. Then 5.5 ml of 96% H_2SO_4 in MeOH was added dropwise. The reaction mixture was stirred at 100° C under a condenser overnight.

After that, distilled water was added to the reaction mixture and a precipitate occurred. The precipitate was filtered, washed with distilled water, and used for the next step without further purification. Yield was 5 g (90%).

3.3.2 Synthesis of IMD-22

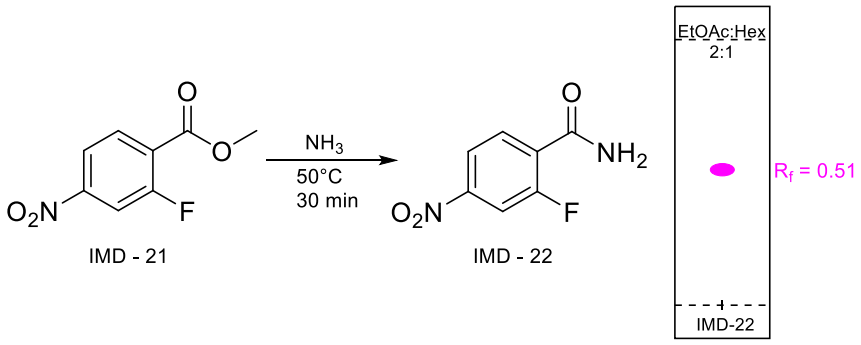

Reagents	**m(mg)/V(ml)**	**n (mmol)**	**MW (g/mol)**	**Equivalents**
IMD - 21	3 g	15.5	199.03	1.0
NH_3 solution in water (25% m/m)	75.0 ml		17.03	

IMD-21 (15.5 mmol) was dissolved in NH_3 solution in water (25% m/m) and was stirred at 50° C for 30 minutes.

The reaction mixture was acidified with 1M HCl. The formed precipitate was filtered and washed with distilled water. 600 mg (21%) of the pure compound was gained. Loss of the product was caused by overpressure and leakage. HPLC-MS showed one peak of 100% purity.

3.4 Synthesis of IMD 2 series – complete reaction scheme of the first derivate

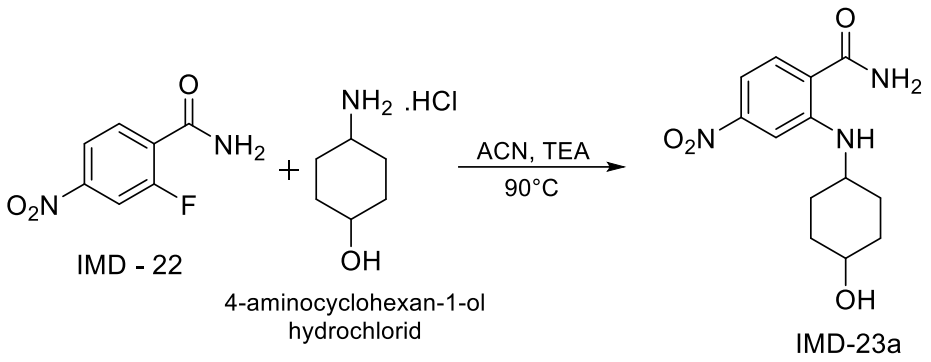

IMD - 22

4-aminocyclohexan-1-ol hydrochlorid

IMD-23a

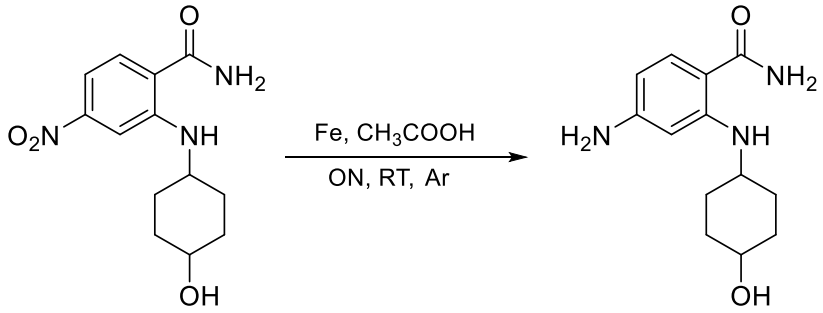

IMD-23a

IMD-23b

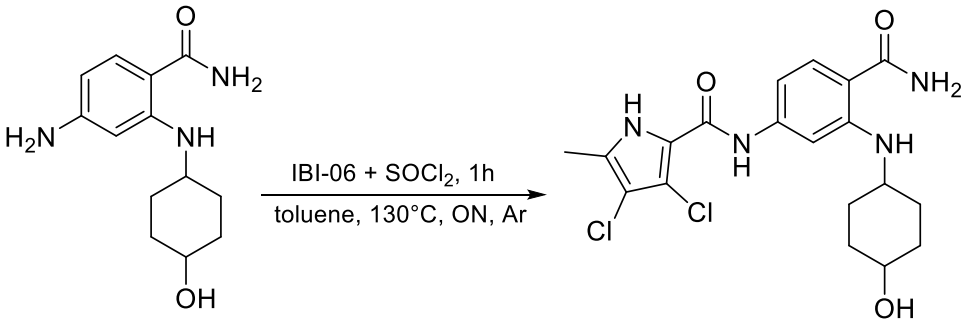

IMD-23b

IMD-23c

3.4.1 Synthesis of IMD-23a

First attempt:

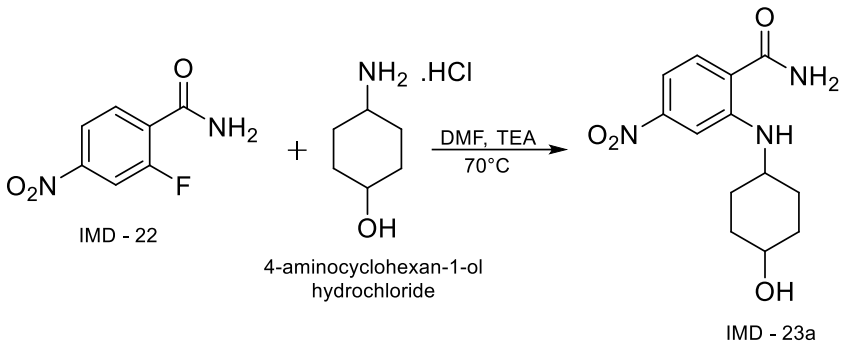

Reagents	m(mg)/V(ml)	n (mmol)	MW (g/mol)	Equivalents
IMD - 22	106 mg	0.6	184.00	1.0
Aminocyklohexanol	256 mg	1.6	151.63	2.7
DMF	2.5 ml		41.05	
TEA	0.8 ml	5.8	101.19	9.7

IMD-22 (0.6 mmol) and 4-aminocyclohexan-1-ol (1.6 mmol) were dissolved in anhydrous DMF. The reaction mixture was stirred overnight at 70° C. The reaction went very slowly, so 9.7 equivalents of anhydrous TEA were added. The reaction was stopped and analyzed after one week.

The reaction mixture was concentrated under reduced pressure. Column chromatography (DCM:MeOH 9:1) was performed (Figure 18 represents the TLC of the mixture before column chromatography). The residue was dissolved in EtOAc, and washed with distilled water, saturated $NaHCO_3$, and brine. The organic phase was dried over Na_2SO_4 and evaporated under reduced pressure. The yield was so low, that this reaction had to be repeated.

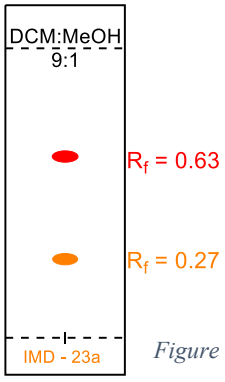

Figure 18 TLC of IMD-23a (red spot represents impurity of DMF).

While investigating the cause of the low yield, it was observed that the same peak appears on HPLC- MS of IMD-23a, IMD-24a, and IMD-25a (Figure 19).

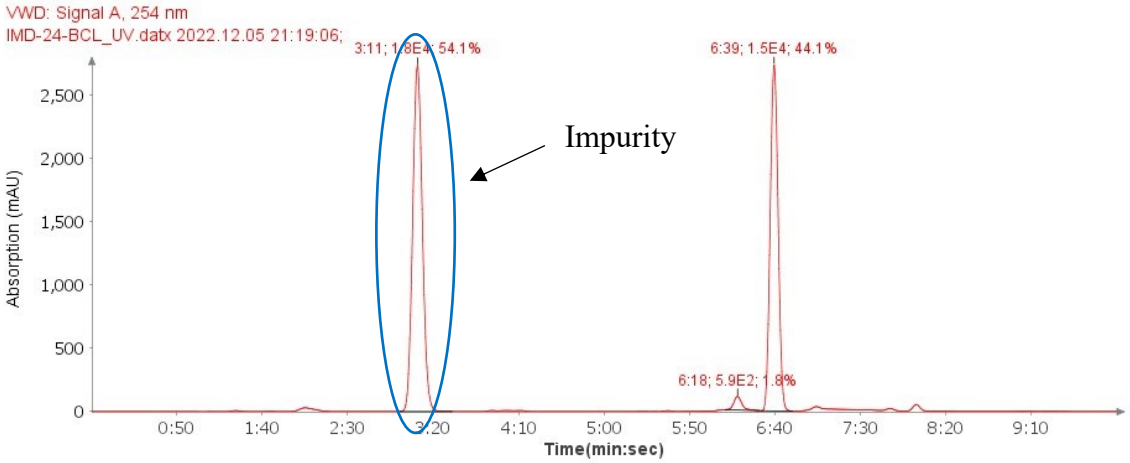

Figure 19 HPLC of impurity in reactions of IMD-23a, IMD-24a, and IMD-25a.

The impurity was separated and analyzed (Figure 20).

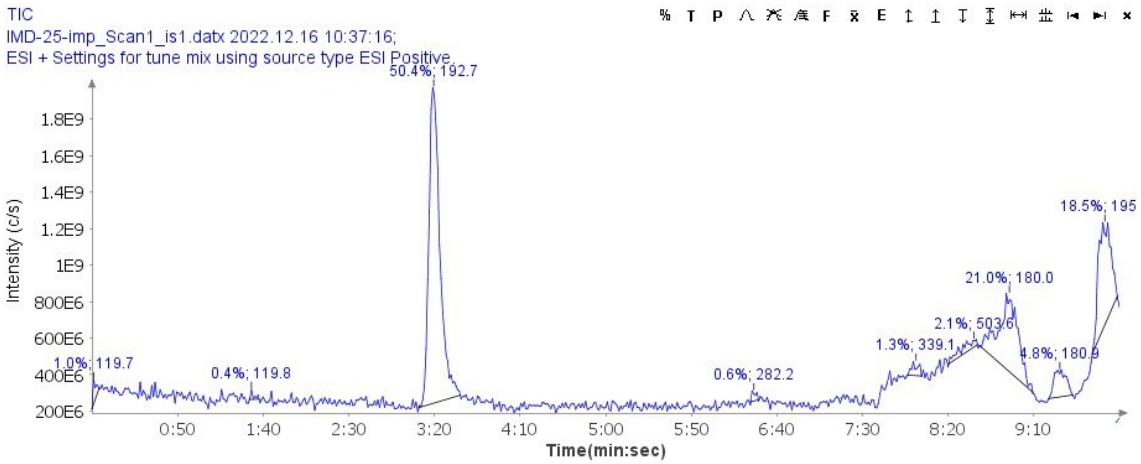

Figure 20 MS of isolated impurity of IMD-23a, IMD-24a and IMD-25a.

It was found that the impurity was from DMF. This was due to moisture in the solvent which led to hydrolysis to formic acid and dimethylamine (Figure 21) according to the equation[46]:

$$HCON(CH_3)_2 + H_2O \longrightarrow HCOOH + (CH_3)_2NH$$

Figure 21 Equation of hydrolysis of DMF. Taken from Juillard J.[46]

Most likely, an impurity was formed by dimethylamine substituting fluor in IMD-22 (Figure 22):

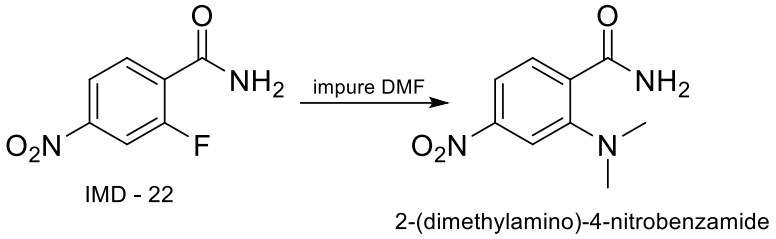

Figure 22 Assumed forming of IMD series 2 impurity.

Second attempt:

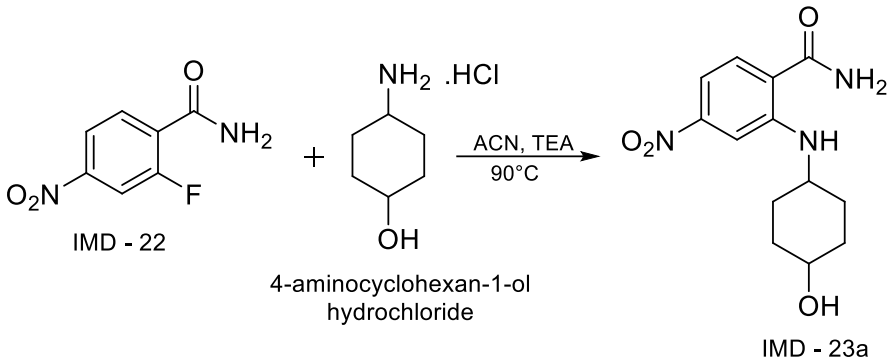

Reagents	**m(mg)/V(ml)**	**n (mmol)**	**MW (g/mol)**	**Equivalents**
IMD – 22	106 mg	0.6	184.00	1.0
Aminocyclohexanol	346 mg	2.3	151.63	3.8
ACN	2.5 ml		41.05	
TEA	0.8 ml	5.8	101.19	9.7

IMD-22 (0.6 mmol) and 4-aminocyclohexan-1-ol (2.3 mmol) were suspended in anhydrous ACN. 9.7 equivalents (0.8 ml) of anhydrous TEA were added. The reaction mixture was stirred overnight at 90° C under a condenser. Figure 23 shows the reaction status after 2h with 9.7 equivalents of TEA. 25 more equivalents (2 ml) of anhydrous TEA were added sequentially to increase reactivity.

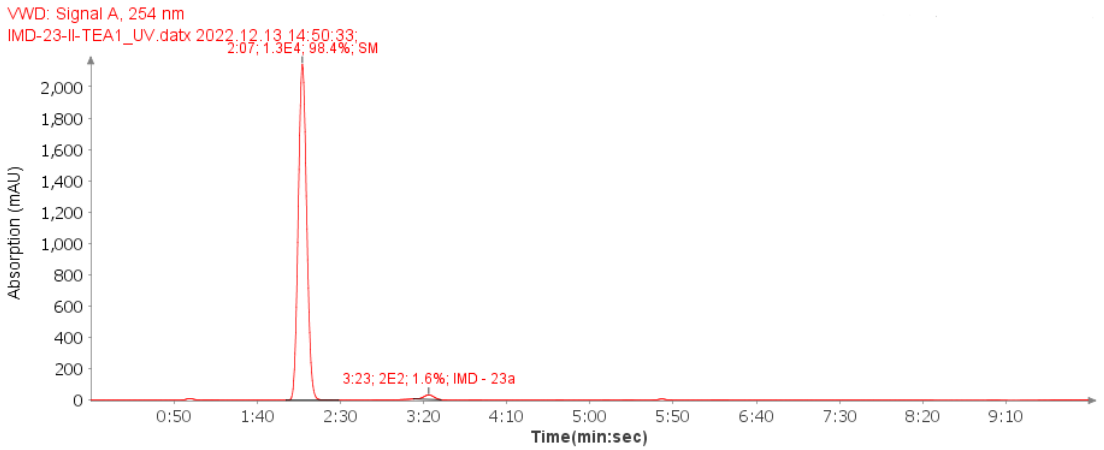

Figure 23 IMD-23a 2H after adding 10 equivalents of TEA (13,12,2022).

TLC analysis proved unfinished synthesis. 4 equivalents of 4-aminocyclohexan-1-ol were added (Figure 24).

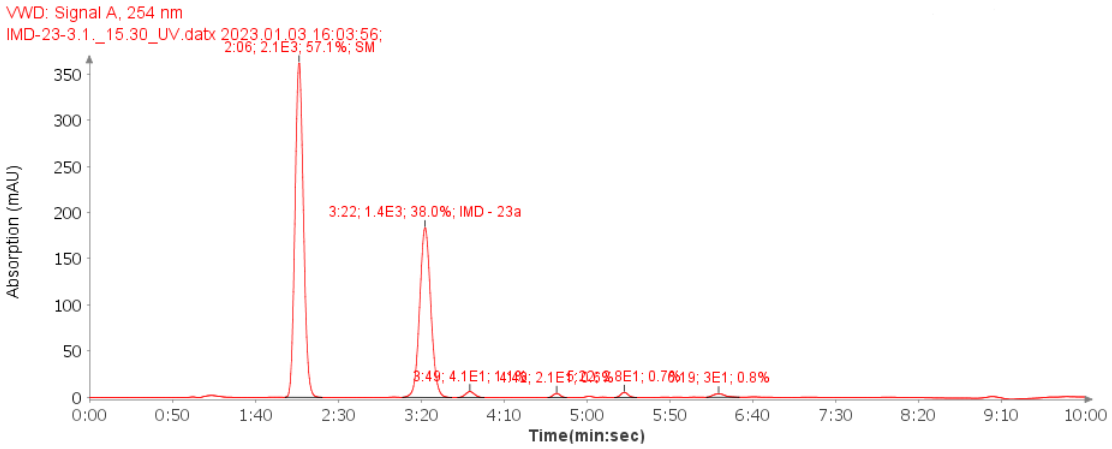

Figure 24 IMD-23a three weeks and 2 more ml of TEA later (3.1.2023).

The reaction was stopped on 42% of the starting material and 53% of the product. It was unsuccessful to separate the product by any available method (Figure 25).

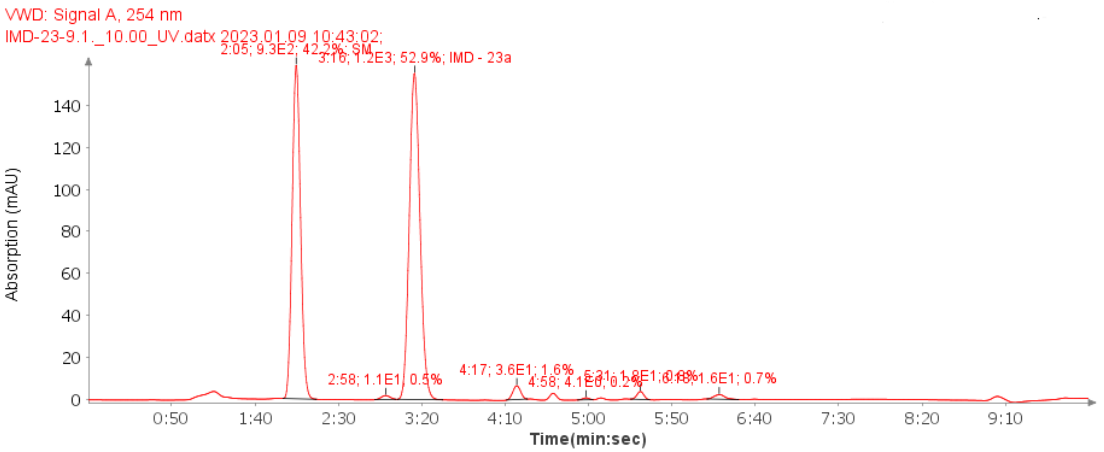

Figure 25 IMD-23a 9.1.2023.

3.5 Synthesis of IMD 2 series – complete reaction scheme of the second derivate

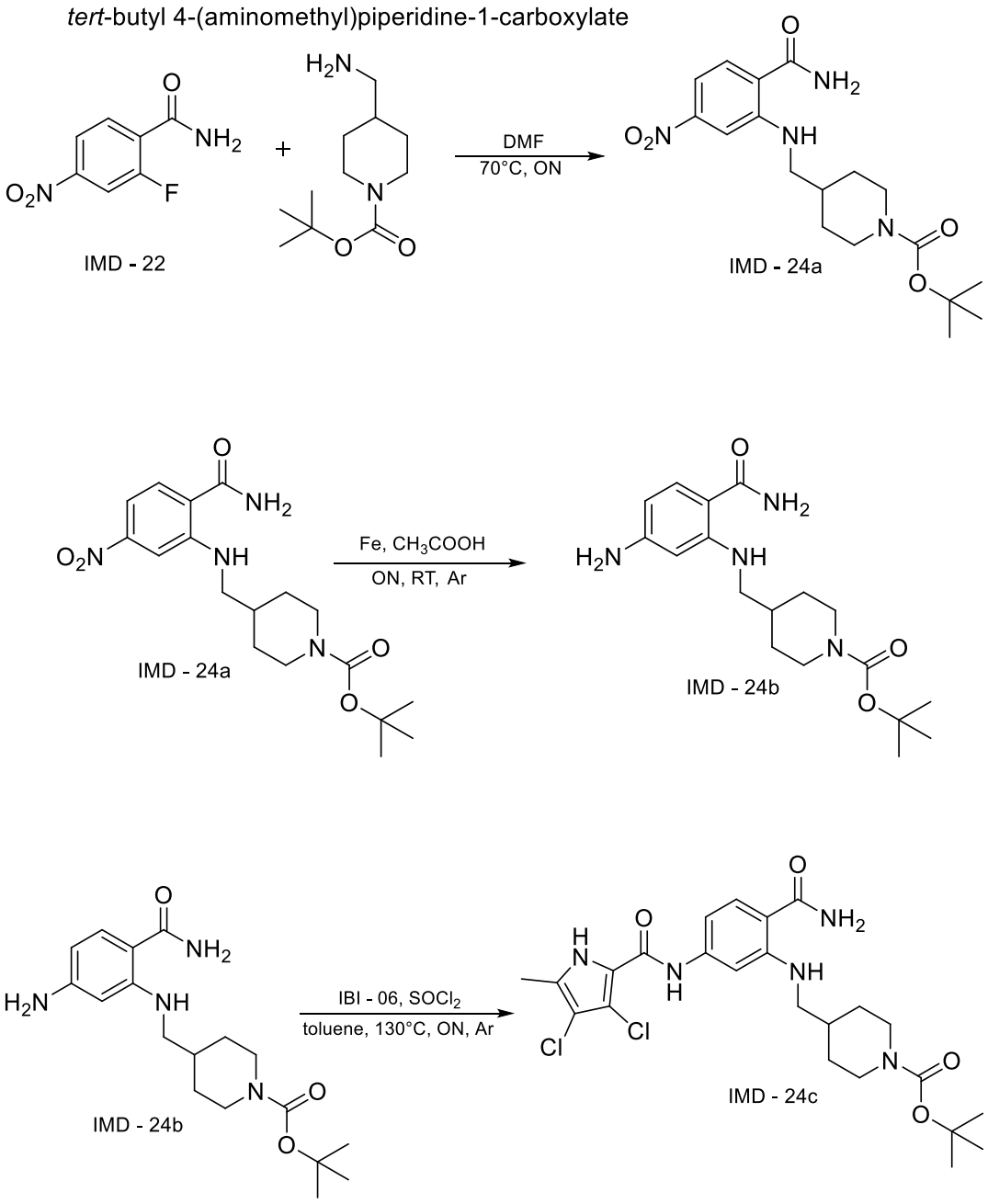

3.5.1 Synthesis of IMD-24a

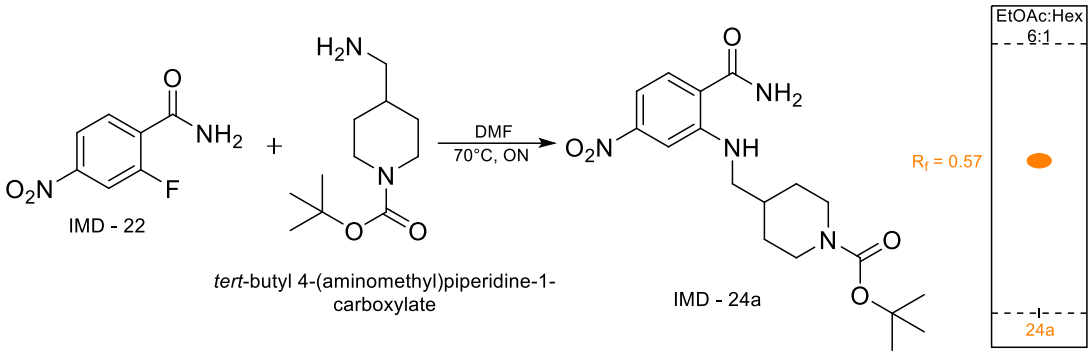

Reagents	m(mg)/V(ml)	n (mmol)	MW (g/mol)	Equivalents
IMD - 22	103 mg	0.6	184.00	1.0
BOC protected compound	250 mg	1.2	214.31	2.0
DMF	3.0 ml		73.09	

IMD-22 (0.6 mmol) and 1-(4-(aminomethyl) piperidine-1-yl)-3,3-dimethylbutan-1-one (1.2 mmol) were dissolved in anhydrous DMF. The reaction mixture was stirred overnight at 70° C.

The reaction was then concentrated under reduced pressure. The residue was dissolved in EtOAc, transferred to the separating funnel, and washed with distilled water, saturated $NaHCO_3$ and brine. The organic phase was dried over Na_2SO_4, filtered, and concentrated under reduced pressure.

The mixture was polluted by the impurity mentioned earlier (Figure 22). Column chromatography was performed using mobile phase EtOAc:Hex 6:1. Yield was 68 mg (32%). HPLC-MS was done with the result of one peak with 100% purity. A purified compound was used for the next step.

The product had the structure of solidified oil which varies in colour. Goes from red (concentrated) through orange to yellow (diluted). It is possibly caused by electron density, which shifts the visible spectrum to red when concentrated.

3.5.2 Synthesis of IMD-24b

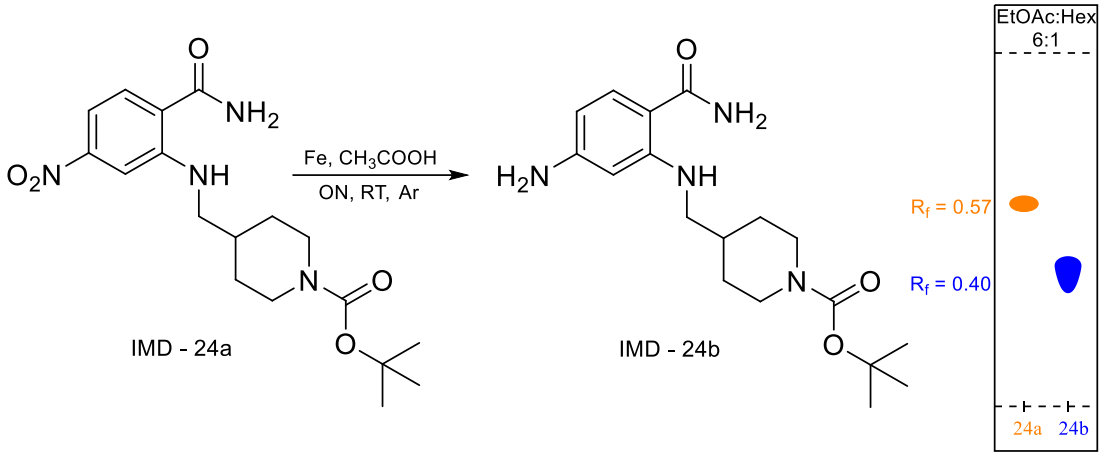

Reagents	**m(mg)/V(ml)**	**n (mmol)**	**MW (g/mol)**	**Equivalents**
IMD - 24a	68 mg	0.2	378.19	1
Fe	151 mg	2.7	55.85	13.5
CH_3COOH	2.5 ml		60.05	

IMD-24a (0.2 mmol) was dissolved in neat CH_3COOH, and Fe (2.7 mmol) was added. The reaction was stirred overnight at room temperature under an argon atmosphere. The reaction mixture had a white colour. After removing the argon and opening the septum, the reaction mixture slowly turned brown.

The crude reaction mixture was neutralized with NH_3 solution in water (25% m/m), transferred to a separating funnel and extracted with ethyl acetate (200+100ml). The organic phase was washed with distilled water, saturated $NaHCO_3$, and brine, dried over anhydrous Na_2SO_4 and concentrated under reduced pressure. Absorption of UV on TLC went from 254nm to 366nm. HPLC- MS showed 88.1% purity. Yield was 63 mg (100%).

3.5.3 Synthesis of IMD-24c

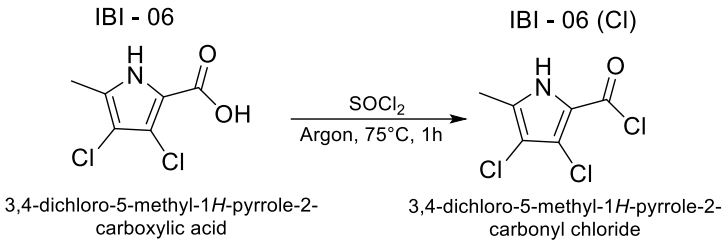

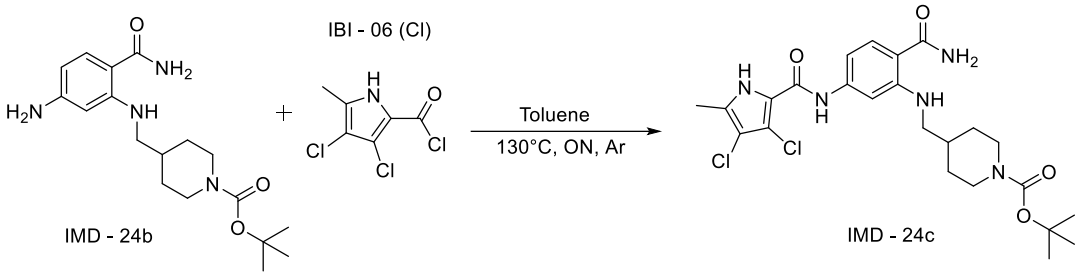

Reagents	**m(mg)/V(ml)**	**n (mmol)**	**MW (g/mol)**	**Equivalents**
IBI-06	49 mg	0.3	194.011	1.5
$SOCl_2$	1.0 ml	13.8	118.97	74.0
IMD - 24b	64 mg	0.2	348.22	1.0
Toluene	5.0 ml		92.14	

IBI-06 (0.3 mmol) was stirred in excess of $SOCl_2$ at 75° C for 1h under an argon atmosphere. $SOCl_2$ was then evaporated, using a water pump, and dried for 10 minutes under reduced pressure. IMD-24b (0.2 mmol) and anhydrous toluene were added to IBI-06(Cl) carefully. The reaction mixture was stirred overnight at 130° C under a condenser and an argon atmosphere.

The reaction was unfinished, so more IBI-06 was added (31 mg) and stirred until the next day. After that, the reaction was stopped (the status of the reaction is shown in Figure 26), and the toluene was evaporated. The crude reaction mixture was stirred in anhydrous MeOH overnight to wash. Then the mixture was filtered. Because of the low yield, this reaction has to be repeated.

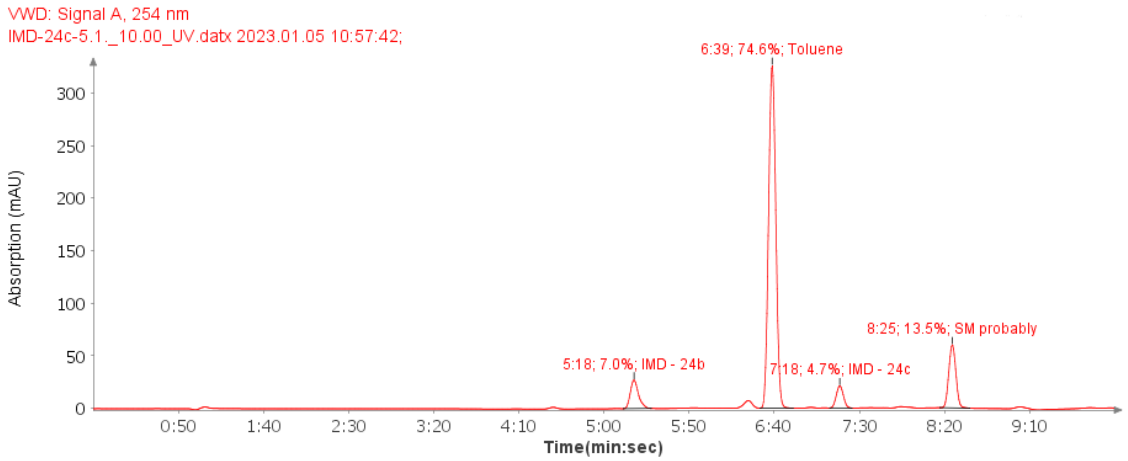

Figure 26 HPLC of the reaction mixture of IMD-24c. SM = IBI-06.

3.6 Synthesis of IMD 2 series – complete reaction scheme of the third derivate

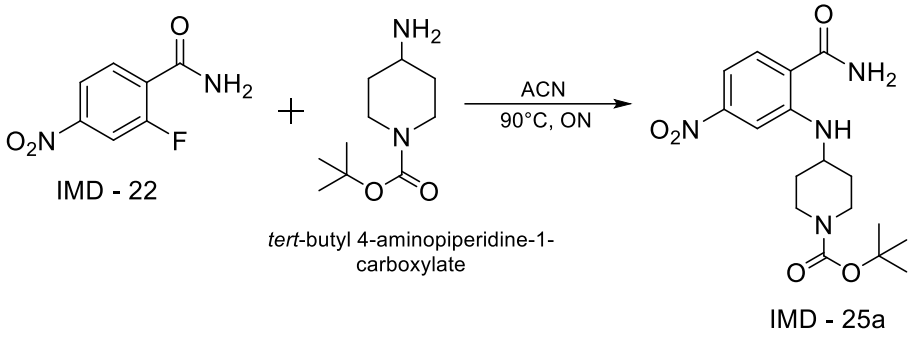

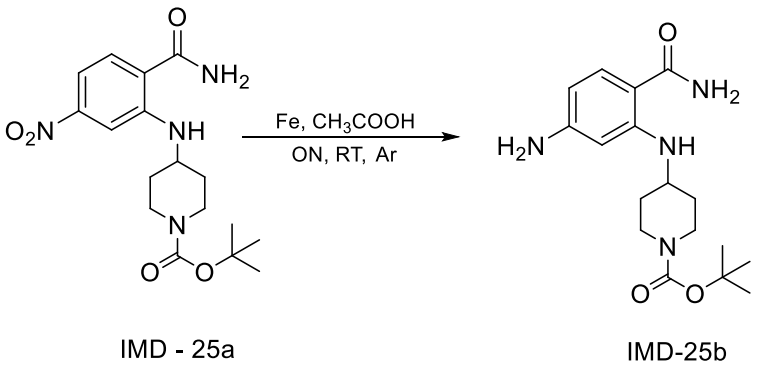

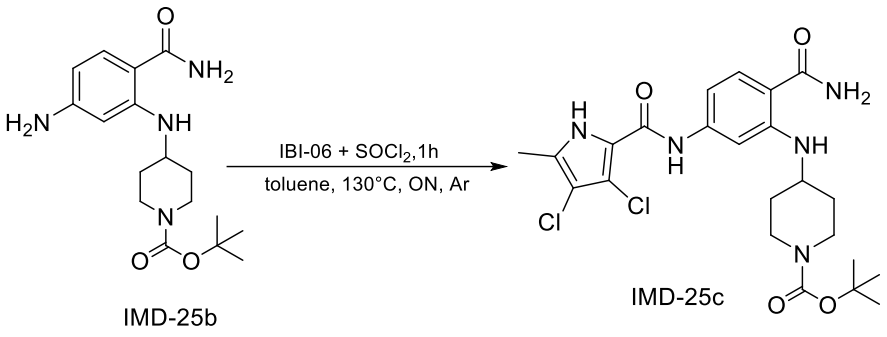

3.6.1 Synthesis of IMD-25a

First attempt:

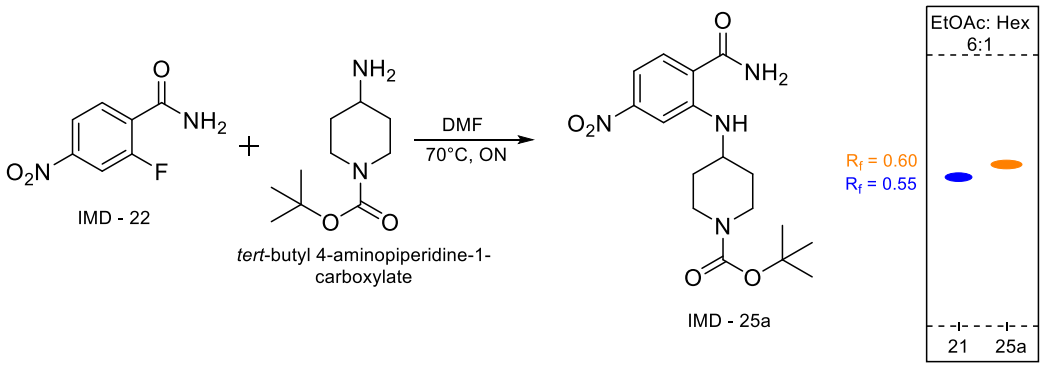

Reagents	m(mg)/V(ml)	n (mmol)	MW (g/mol)	Equivalents
IMD – 22	109 mg	0.6	184.00	1.0
BOC compound	242 mg	1.2	200.15	2.0
DMF	2.5 ml		73.09	

IMD-22 (0.6 mmol) and *tert*-butyl 4-aminopiperidine-1-carboxylate (1.2 mmol) were dissolved in anhydrous DMF. The reaction mixture was stirred overnight at 70° C.

The reaction mixture was then concentrated under reduced pressure. The residue was dissolved in EtOAc, transferred to the separating funnel and washed with distilled water, saturated $NaHCO_3$ and brine. The organic phase was dried over Na_2SO_4, filtered and concentrated under reduced pressure. Because of impurities in DMF mentioned above, only less than 50% of the product has formed.

Column chromatography was done with mobile phase EtOAc:Hex 6:1 to purify the organic phase. It was proceeded to the next step. However, the reduction failed, and the reaction had to be repeated.

Second attempt

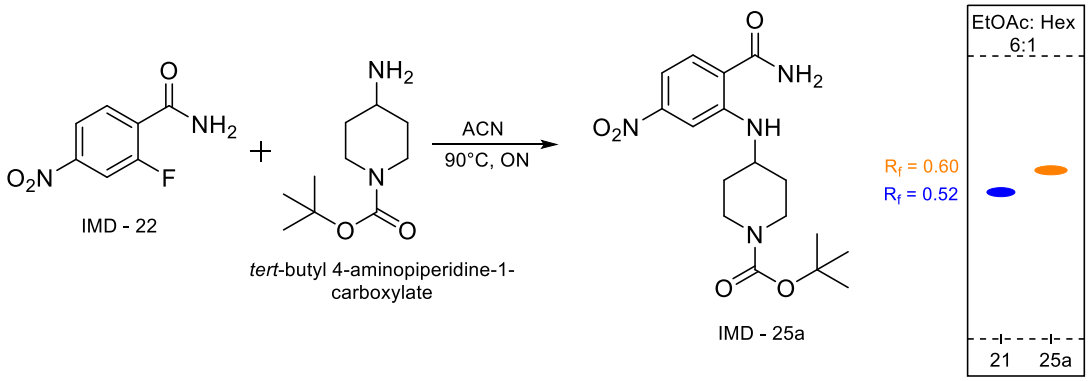

Reagents	m(mg)/V(ml)	n (mmol)	MW (g/mol)	Equivalents
IMD - 22	116 mg	0.6	184.00	1.0
BOC compound	402 mg	1.2	200.15	3.0
Acetonitrile	2.5 ml		41.05	

IMD-22 (0.6 mmol) and *tert*-butyl 4-aminopiperidine-1-carboxylate (1.2 mmol) were suspended in anhydrous ACN. The reaction mixture was stirred overnight at 90° C under a condenser.

The reaction was then concentrated under reduced pressure. The residue was dissolved in EtOAc, transferred to the separating funnel, and washed with distilled water, saturated $NaHCO_3$ and brine. The organic phase was dried over Na_2SO_4, filtered, and concentrated under reduced pressure. However, the purity was insufficient, so column chromatography was chosen for further purification (EtOAc:Hex 6:1). HPLC-MS after column chromatography showed 96.5% purity with residual impurity of IMD-22. This was considered pure enough to proceed with the next step. The yield was 50 mg (23%).

3.6.2 Synthesis of IMD-25b

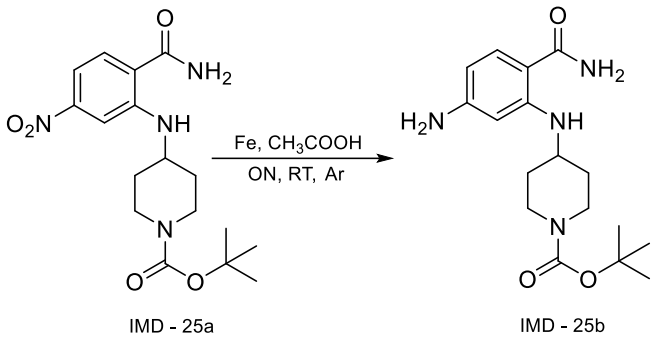

Reagents	**m(mg)/V(ml)**	**n (mmol)**	**MW (g/mol)**	**Equivalents**
IMD - 25a	49 mg	0.1	378.19	1.0
Fe	135 mg	2.4	55.85	24.0
CH_3COOH	4.0 ml		60.05	

IMD-25a (0.1 mmol) was dissolved in neat CH_3COOH, and Fe (2.4 mmol) was added. The reaction was stirred overnight at room temperature under an argon atmosphere. The crude reaction mixture had a white colour. After removing the argon and opening the septum, the reaction mixture slowly turned brown.

The crude reaction mixture was neutralized with NH_3 solution in water (25% m/m), transferred to a separating funnel, and extracted with ethyl acetate (200+100ml). The organic phase was then washed with distilled water, saturated $NaHCO_3$ and brine, dried over Na_2SO_4 and concentrated under reduced pressure. HPLC-MS showed a compound of 97.3% purity. Unfortunately, yield was so low, that this reaction needs to be repeated in the future.

3.7 Compounds' characterizations

^{1}H NMR abbreviations:

ArH – hydrogen of the aromatic ring

BocH – hydrogen of *tert*-butyloxycarbonyl

CONH – amidic hydrogen

eCH3 – methyl ester hydrogen

pCH3 – pyrrole methyl hydrogen

PipH – piperidine hydrogen

PyrH – pyrrole hydrogen

sCH3 – sulfanyl methyl hydrogen

3.7.1 IMD-01

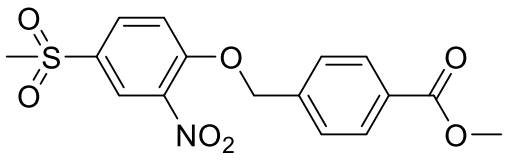

Name: methyl 4-((4-(methylsulfonyl)-2-nitrophenoxy)methyl)benzoate

Appearance: white solid

Molecular weight: 365.36 g/mol

Yield: 68%

Retention factor: 0.68 (EtOAc:Hex 3:1)

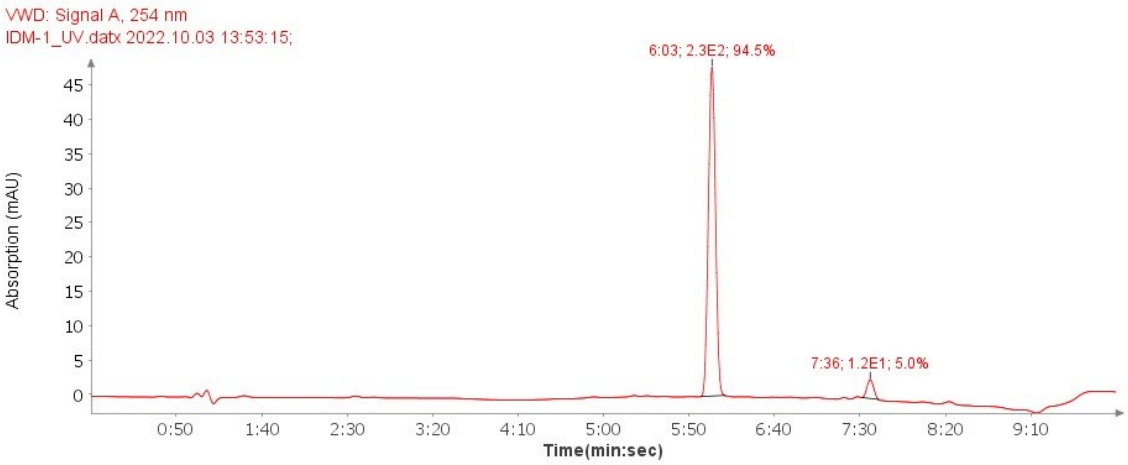

3.7.2 IMD-02

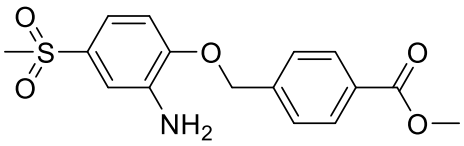

Name: methyl 4-((2-amino-4-(methylsulfonyl)phenoxy)methyl)benzoate

Appearance: beige solid

Molecular weight: 335.37 g/mol

Yield: 96%

Retention factor: 0.73 (EtOAc:Hex 2:1)

HPLC-MS (ESI+, m/z): $[M+H]^+$ 377.1 (adduct with ACN)

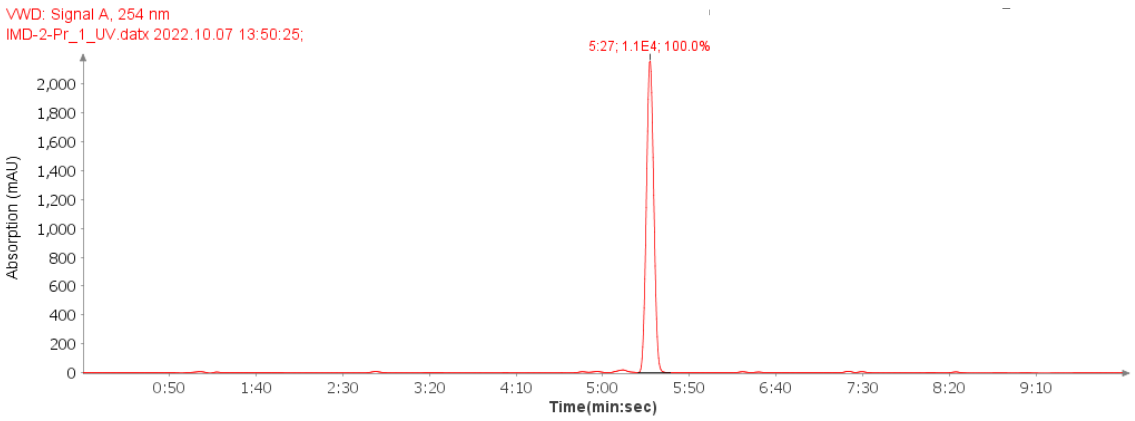

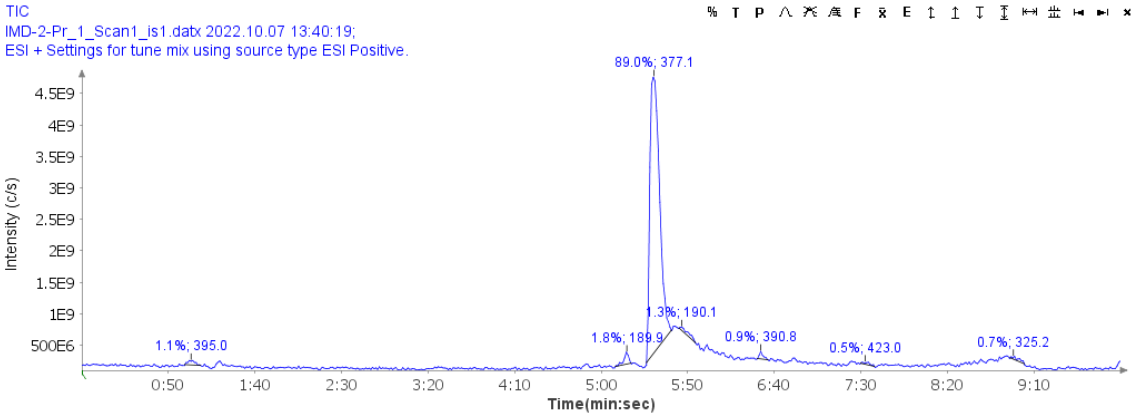

3.7.3 IMD-03

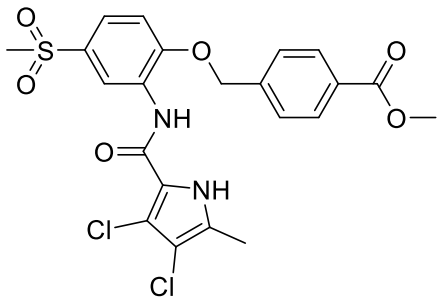

Name: methyl 4-((2-(3,4-dichloro-5-methyl-1*H*-pyrrole-2-carboxamido)-4-(methylsulfonyl)phenoxy)methyl)benzoate

Appearance: beige solid

Molecular weight: 511.37 g/mol

Yield: 56%

Retention factor: 0.25 (DCM:MeOH 49:1)

^{1}H NMR (400 MHz, DMSO-d_6) δ 12.42 (s, 1H, CONH), 9.17 (s, 1H, PyrH), 8.95 (d, 1H, ArH), 8.07 – 8.00 (m, 2H, ArH), 7.75 – 7.66 (m, 3H, 1 ArH), 7.47 (d, 1H, ArH), 5.43 (s, 2H, CH_2), 3.89 (s, 3H, eCH_3), 3.19 (s, 3H, sCH_3), 2.22 (s, 3H, pCH_3).

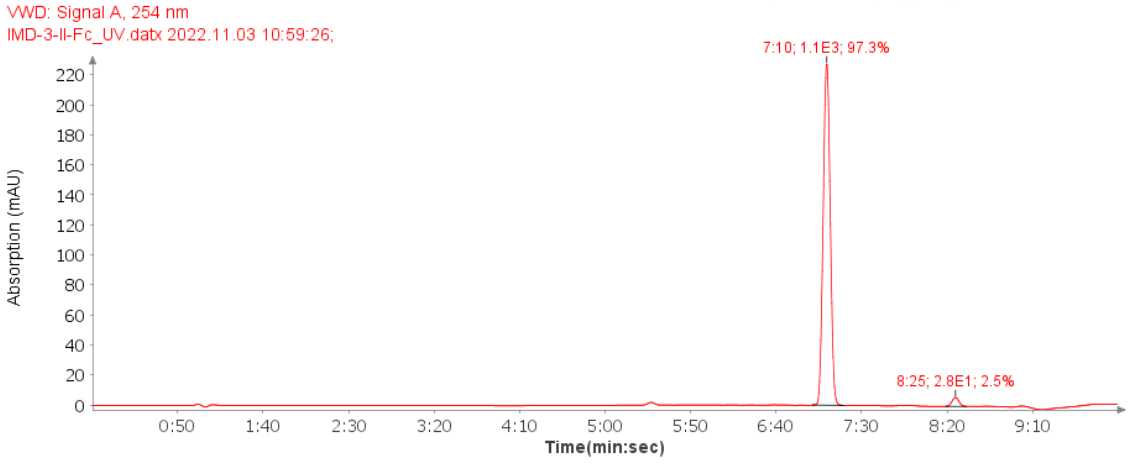

3.7.4 IMD-04

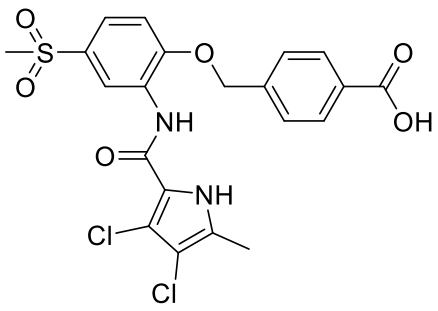

Name: 4-((2-(3,4-dichloro-5-methyl-1*H*-pyrrole-2-carboxamido)-4-(methylsulfonyl)phenoxy)methyl)benzoic acid

Appearance: beige solid

Molecular weight: 497.34 g/mol

Yield: 58%

Retention factor: IMD-04 was sitting at the start (DCM:MeOH 9:1)

HPLC-MS (ESI+, m/z): $[M+H]^+$ 496.4

^{1}H NMR (400 MHz, DMSO-d_6) δ 13.09 (s, 1H, COOH), 12.42 (s, 1H, CONH), 9.17 (s, 1H, PyrH), 8.95 (d, 1H, ArH), 8.04 – 7.97 (m, 2H, ArH), 7.73 – 7.65 (m, 3H, 1 ArH + 2 ArH),7.47 (d, 1H, ArH), 5.42 (s, 2H, CH_2), 3.18 (s, 3H, sCH_3), 2.22 (s, 3H, pCH_3).

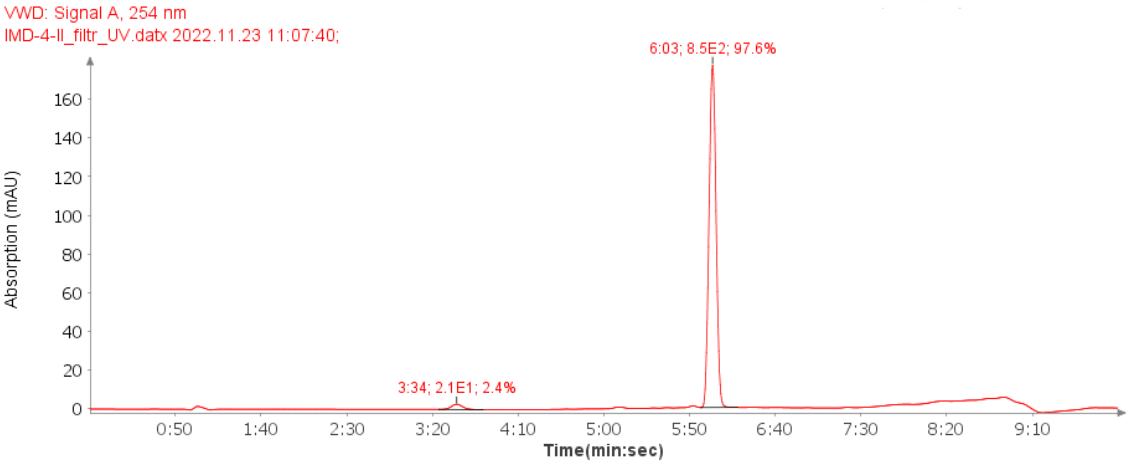

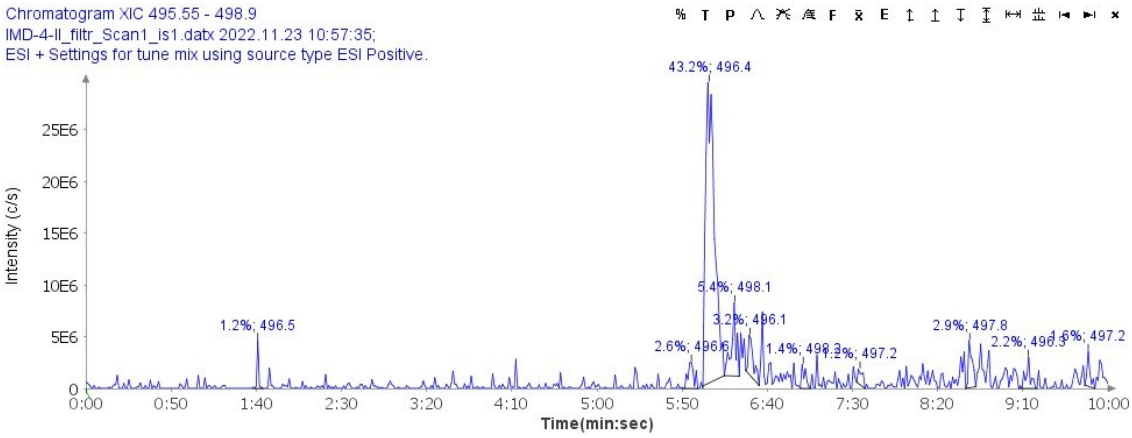
Chromatogram XIC 495.55 - 498.9
IMD-4-II_filtr_Scan1_is1.datx 2022.11.23 10:57:35;
ESI + Settings for tune mix using source type ESI Positive.
Intensity (c/s)
25E6
20E6
15E6
10E6
5E6
0
0:00
0:50
1:40
2:30
3:20
4:10
5:00
5:50
6:40
7:30
8:20
9:10
10:00
Time(min:sec)
43.2%; 496.4
5.4%; 498.1
3.2%; 496.1
1.2%; 496.5
2.6%; 496.6
1.4%; 498.2
1.2%; 497.2
2.9%; 497.8
2.2%; 496.5
1.6%; 497.2

3.7.5 IMD-11

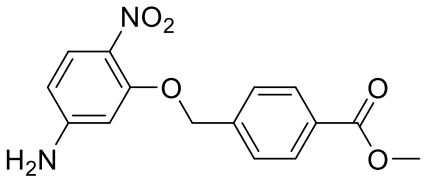

Name: methyl 4-((5-amino-2-nitrophenoxy)methyl)benzoate

Appearance: orange solid

Molecular weight: 302.29 g/mol

Yield: 53%

Retention factor: 0.63 (EtOAc:Hex 2:1)

HPLC-MS (ESI+, m/z): $[M+H]^+$ 288.4 (loss of CH_3)

^{1}H NMR (400 MHz, DMSO-d_6) δ 8.05 – 7.96 (m, 2H, ArH), 7.76 (dd, 1H, 1 ArH), 7.72-7.66 (m, 3H, 1 ArH + 2 ArH), 6.71 (d, 1H, ArH), 6.53 (s, 2H, NH_2), 5.35 (s, 2H, CH_2), 3.86 (s, 3H, eCH_3).

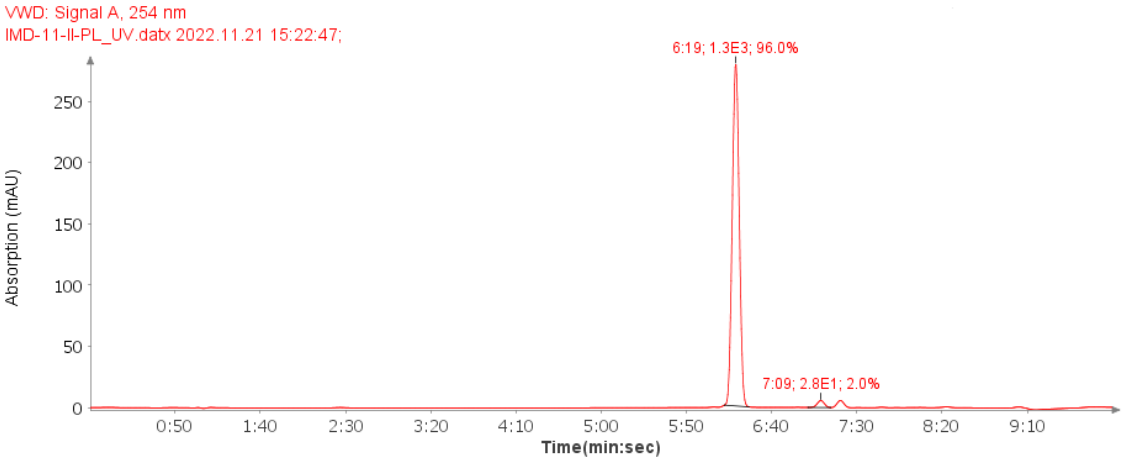

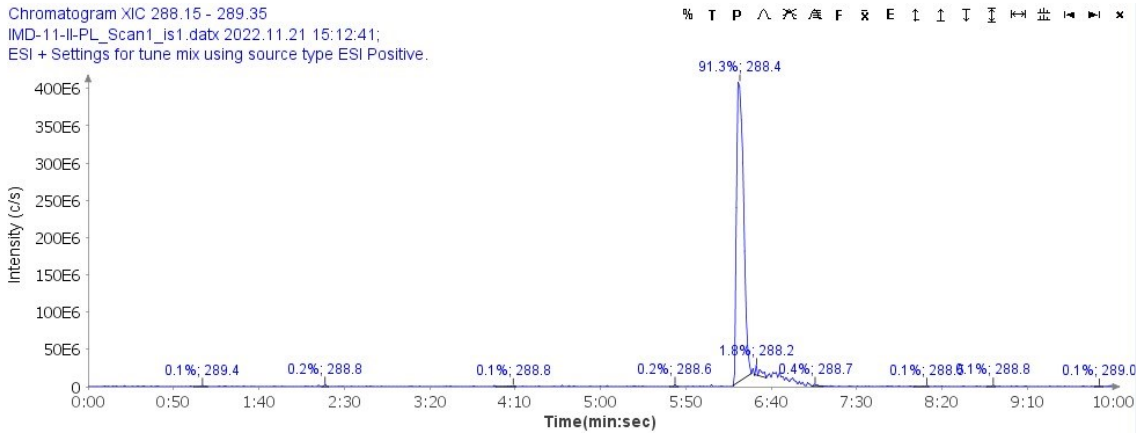

3.7.6 IMD-12

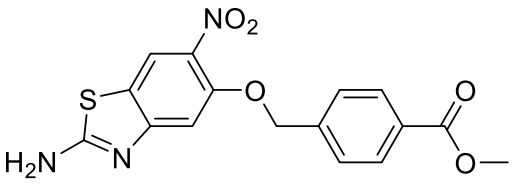

Name: methyl 4-(((2-amino-6-nitrobenzo[d]thiazol-5-yl)oxy)methyl)benzoate

Appearance: orange solid

Molecular weight: 359.36 g/mol

Yield: 36%

Retention factor: unknown

3.7.7 IMD-21

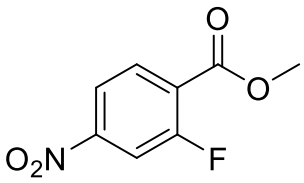

Name: methyl 2-fluoro-4-nitrobenzoate

Appearance: white fluffy solid

Molecular weight: 199.14 g/mol

Yield: 90 %

Retention factor: 0.68 (EtOAc:Hex 2:1)

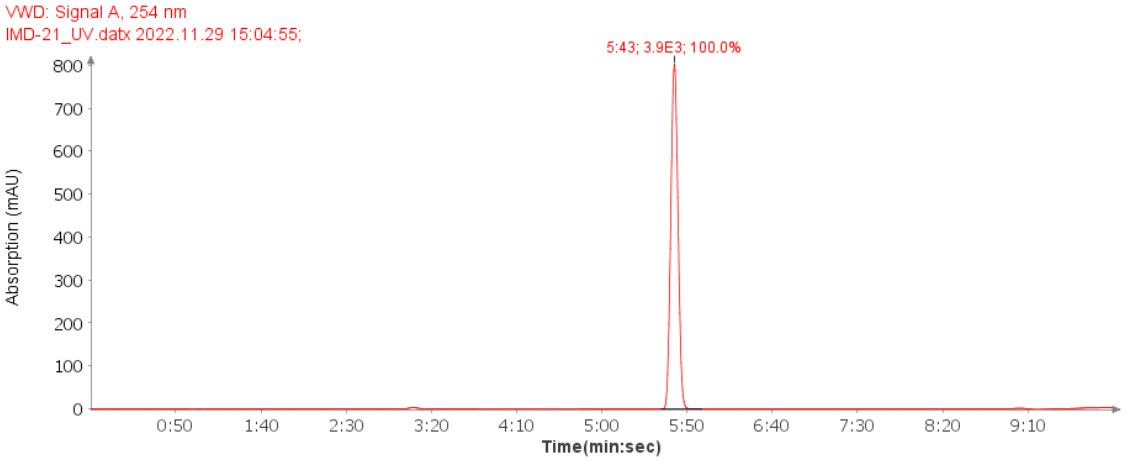

3.7.8 IMD-22

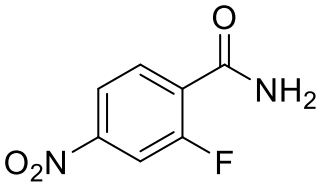

Name: 2-fluoro-4-nitrobenzamide

Appearance: white fluffy solid

Molecular weight: 184.13 g/mol

Yield: 21 %

Retention factor: 0.51 (EtOAc:Hex 2:1)

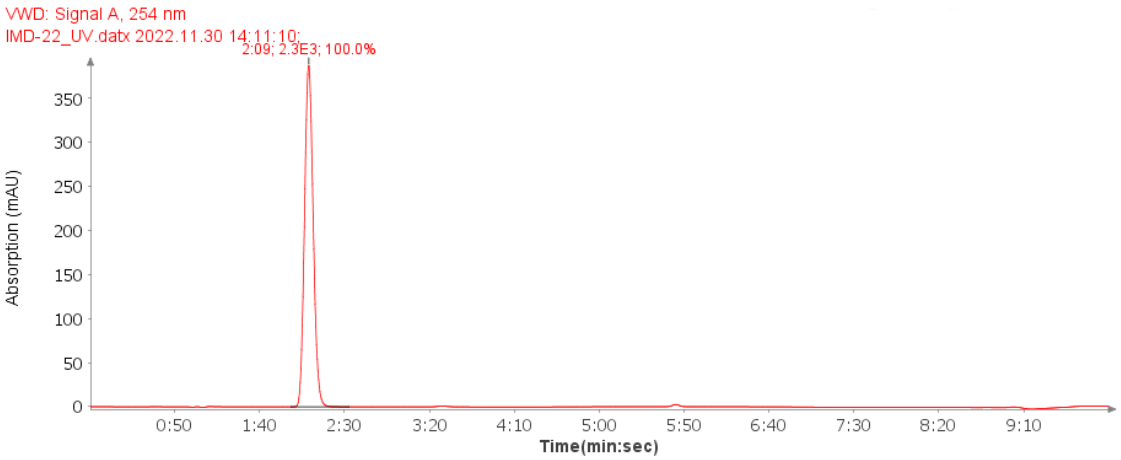

3.7.9 IMD-24a

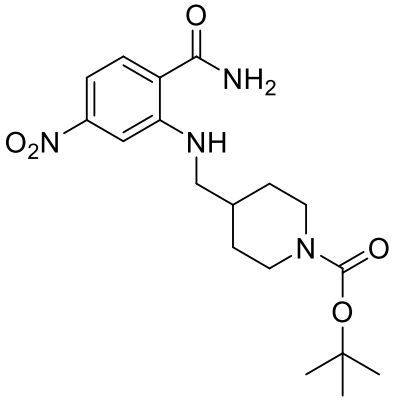

Name: *tert*-butyl 4-(((2-carbamoyl-5-nitrophenyl)amino)methyl)piperidine-1-carboxylate

Appearance: yellow-orange-red solidified oil

Molecular weight: 378.43 g/mol

Yield: 32 %

Retention factor: 0.57 (EtOAc:Hex 6:1)

^{1}H NMR (400 MHz, $CDCl_3$) δ 8.41 (t, 1H, NH), 8.16 (s, 1H, CONH), 7.81 (d, 1H, ArH), 7.56 (s, 1H, CONH), 7.37 (d, 1H, ArH), 7.29 (dd, 1H, ArH), 3.96 (d, 2H, CH_2), 3.11 (t, 2H, PipH), 2.81 – 2.61 (m, 1H, PipH), 1.70 (d, 2H, PipH), 1.39 (s, 9H, BocH), 1.10 (qd, 2H, PipH).

HPLC-MS (ESI+, m/z): $[M+H]^+$ 279.5 (loss of *tert*-butoxycarbonyl)

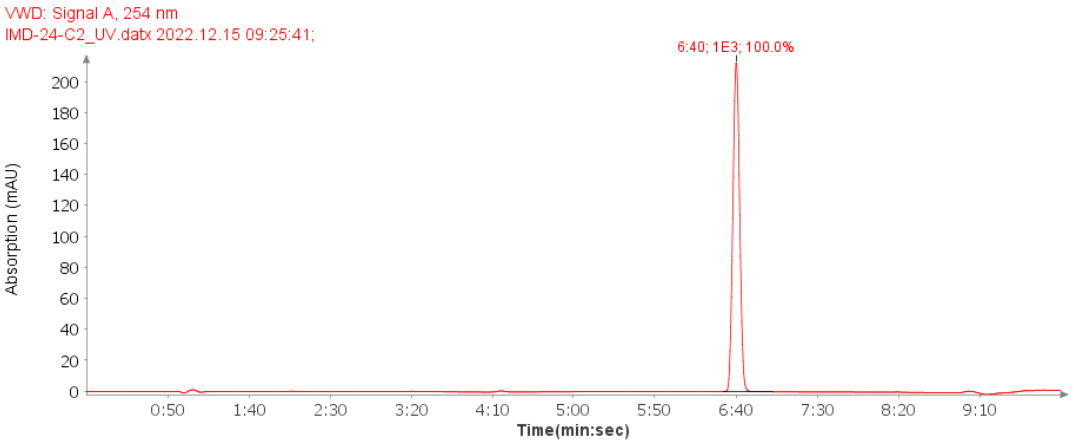

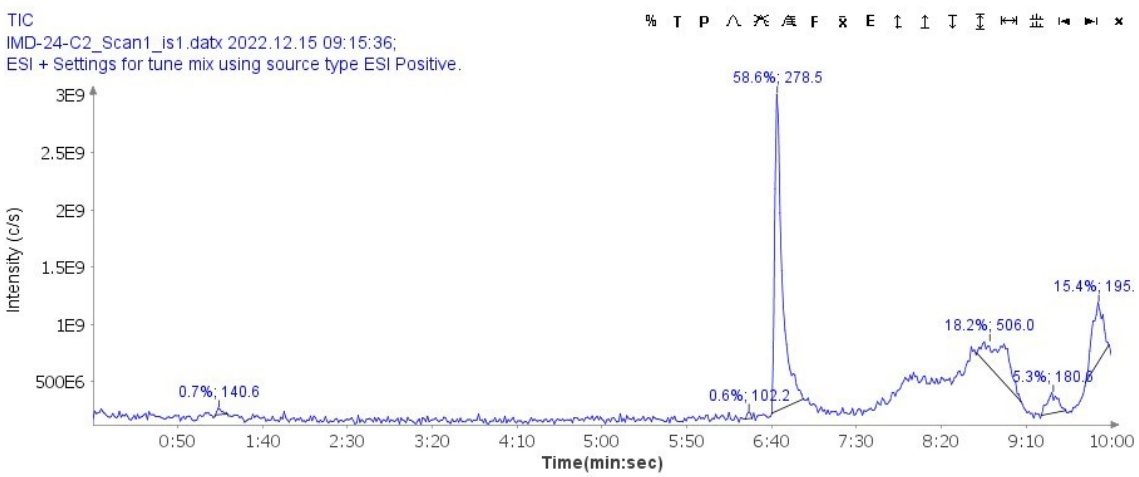
TIC
IMD-24-C2_Scan1_is1.datx 2022.12.15 09:15:36;
ESI + Settings for tune mix using source type ESI Positive.
58.6%; 278.5
15.4%; 195.
18.2%; 506.0
5.3%; 180.8
0.7%; 140.6
0.6%; 102.2
3E9
2.5E9
2E9
1.5E9
1E9
500E6
Intensity (c/s)
0:50
1:40
2:30
3:20
4:10
5:00
5:50
6:40
7:30
8:20
9:10
10:00
Time(min:sec)

3.7.10 IMD-24b

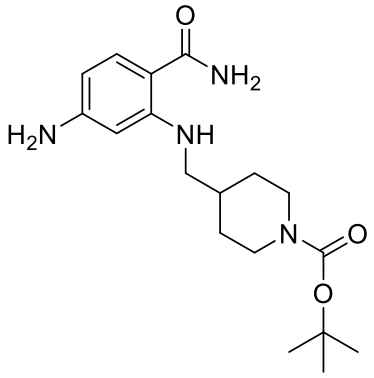

Name: *tert*-butyl 4-(((5-amino-2-carbamoylphenyl)amino)methyl)piperidine-1-carboxylate

Appearance: yellow-orange-red solidified oil

Molecular weight: 348.45 g/mol

Yield: 100 %

Retention factor: 0.40 (EtOAc:Hex 6:1)

HPLC-MS (ESI+,m/z): $[M+H]^+$ 248.7 (loss of *tert*-butoxycarbonyl)

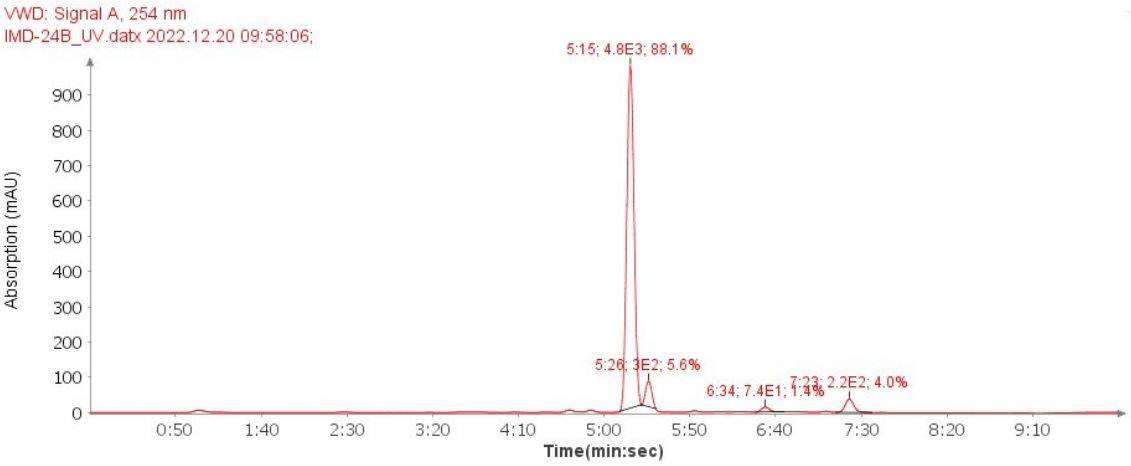

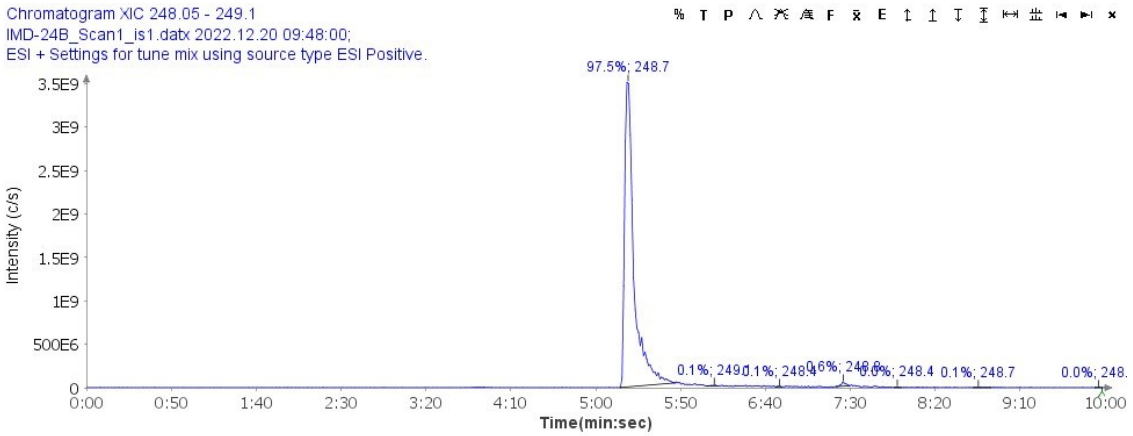
Chromatogram XIC 248.05 - 249.1
IMD-24B_Scan1_is1.datx 2022.12.20 09:48:00;
ESI + Settings for tune mix using source type ESI Positive.
97.5%; 248.7
0.1%; 249
0.1%; 248.4
0.6%; 248.6
0.0%; 248.4
0.1%; 248.7
0.0%; 248.
Intensity (c/s)
3.5E9
3E9
2.5E9
2E9
1.5E9
1E9
500E6
0
0:00
0:50
1:40
2:30
3:20
4:10
5:00
5:50
6:40
7:30
8:20
9:10
10:00
Time(min:sec)

3.7.11 IMD-25a

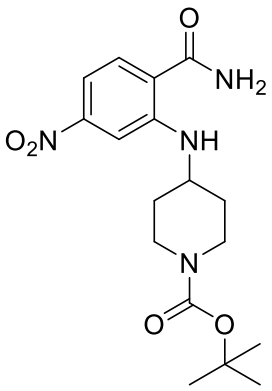

Name: *tert*-butyl 4-((2-carbamoyl-5-nitrophenyl)amino)piperidine-1-carboxylate

Appearance: yellow-orange-red solidified oil

Molecular weight: 364.40 g/mol

Yield: 23 %

Retention factor: 0.60 (EtOAc:Hex 6:1)

HPLC-MS (ESI+, m/z): $[M+H]^+$ 264.8 (loss of *tert*-butoxycarbonyl)

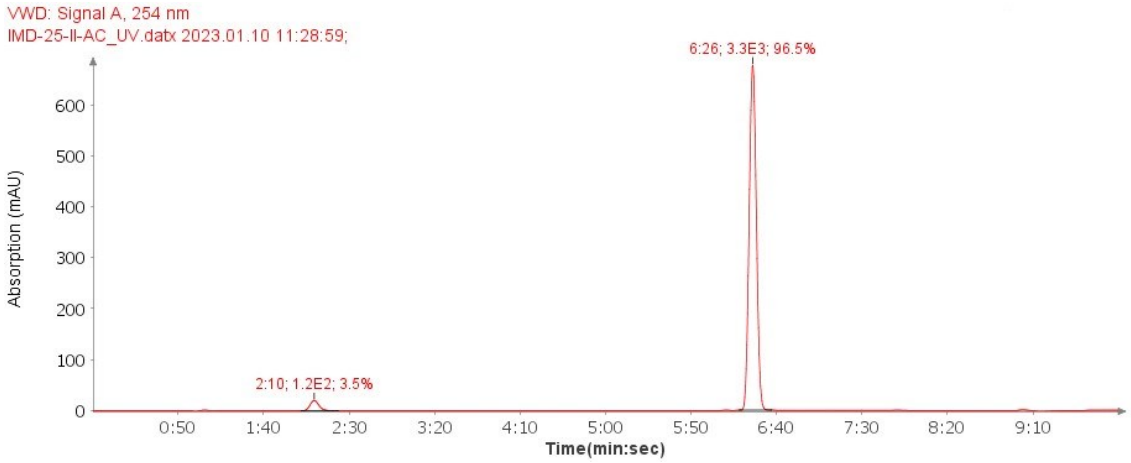

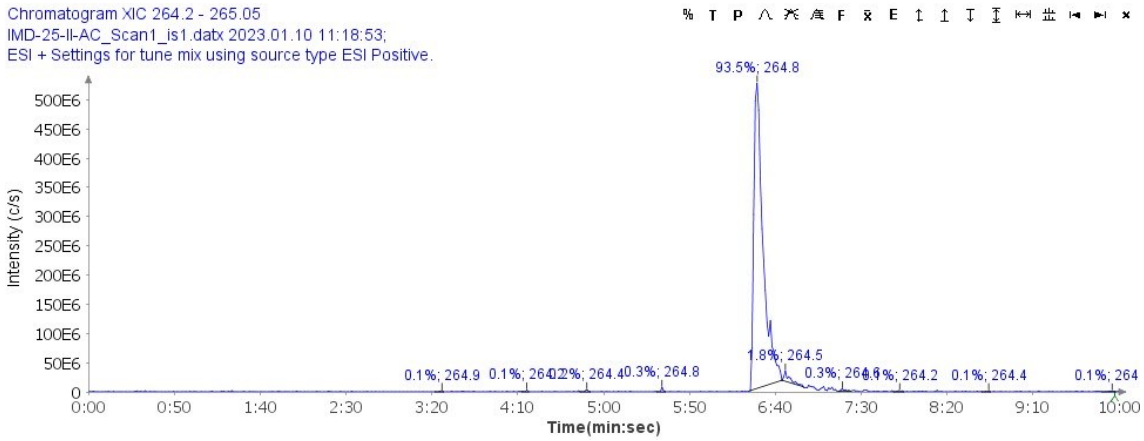

IMD-25b

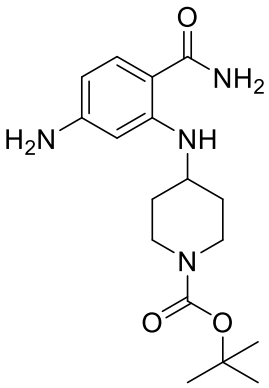

Name: *tert*-butyl 4-((5-amino-2-carbamoylphenyl)amino)piperidine-1-carboxylate

Appearance: yellow-orange-red solidified oil

Molecular weight: 334.42 g/mol

Yield: n.a.

Retention factor: n.a.

HPLC-MS (ESI+, m/z): $[M+H]^+$ 334.9

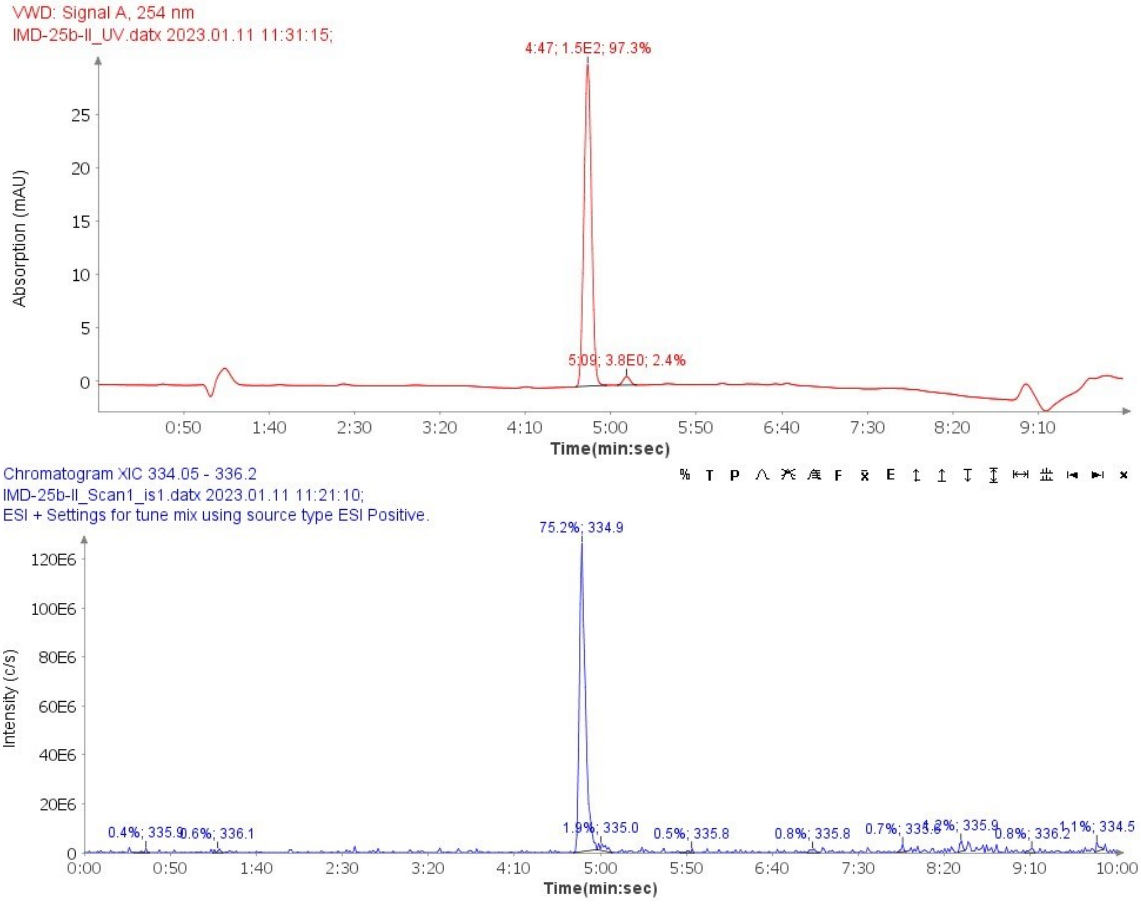

4. Methods

4.1 General and instrumentation

All products were dried to constant weight using an oven set to 55° C.

Chemicals were acquired from Apollo Scientific (Stockport, UK), Asta-Tech (Bristol, PA, USA), Combi-Blocks (San Diego, CA, USA), Fluorochem (Hadfield, UK) Sigma-Aldrich (St.Louis, MO, USA) and were used without prior purification. Solvents were acquired from Carlo Erba (Milan, Italy), Gran-Mol (Zagreb, Croatia) and Merck (Darmstadt, Germany). Solvents for HPLC-MS analysis were of HPLC grade. The solvents for synthesis were anhydrous (HPLC grade).

Reactions were monitored using HPLC-MS as a main tool, and TLC. When these two methods identically claimed that the compound was pure, ^{1}H NMR was done for selected substances.

Thin layer chromatography was carried out on silica gel 60 F_{254} aluminium plates (0.25 mm) supplied by Merck (Darmstadt, Germany), using visualization with UV light (254 and 366 nm) and ninhydrin.

Column chromatography was performed on silica 60 with particle size 240–400 mesh.

Analytical reversed-phase HPLC/UV/MS analyses were performed on a 1260 Infinity II LC system (Agilent Technologies Inc., Santa Clara, CA, USA) using Waters XBridge C18 column (3.5 mm, 4.6 mm × 150 mm) (Waters Crop., Milford, MA, USA), with flow rate of 1.5 ml/min and sample injection volume of 5 µL. The mobile phase contained acetonitrile as solvent A and 0.1% formic acid in 1% acetonitrile in ultrapure water as solvent B. The gradient (defined for solvent A) was: 0-1.0 min, 25%; 1.0-6.0 min, 25%-98%; 6.0-6.5 min, 98%; 6.5-7.5 min, 98%-25%; 7.5-10.5 min, 25%. HPLC was connected to ADVION expression CMSL mass spectrometer (Advion, Ithaca, USA), using a Capillary Temperature of 250° C and Source Gas Temperature of 200° C. A Capillary Voltage of 180V and an ESI Voltage of 2500V were used for the ESI source with negative polarity. A Capillary Voltage of 150V and an ESI Voltage of 3500V were used for the ESI source with positive polarity.

Preparation of the sample for HPLC-MS: Approximately 1 mg of a compound was put into a 2 ml Eppendorf tube and 1 ml of MeOH or ACN (HPLC grade) was added. The compound had to be dissolved. If it was undissolved, ultrasound and heat were used to

dissolve the sample. If ultrasound and heat made no difference in solubility, 100 µl of DMSO was added and the solution was well mixed. 100 µl of this solution was taken away and diluted to the final volume1 ml by the mobile phase composed of 60% ACN and 40% water solution of 0.1% TFA.

^{1}H NMR spectra were recorded on a Bruker VNMR S500 (Varian, Palo Alto, CA, USA) at 400 MHz. The spectra were recorded in DMSO-d_6 at ambient temperature. The chemical shifts were reported as δ values in ppm and were indirectly referenced to tetramethylsilane (TMS) via the solvent signal (2.49 for 1H in DMSO- d_6).

4.2 Topoisomerase IIα inhibition assay

This protocol for testing inhibitory activity against topoIIα was taken over from Skok et al.[31] *Inhibitory activity against topoIIα* was determined with commercially available relaxation assay kits (Inspiralis Limited, Norwich, UK) on PierceTM streptavidin-coated 96-well microtiter plates (Thermo Scientific, Rockford, IL, USA). The plates were rehydrated with wash buffer (20 mM Tris·HCl, 137 mM NaCl, 0.01% w/v BSA, 0.05% v/v Tween 20, pH 7.6) and then biotinylated triplex-forming oligonucleotide dissolved in wash buffer added for 5 min to immobilize. The unbound oligonucleotide was washed off with wash buffer. Next, enzymatic reaction was performed: the reaction volume of 30 µL in buffer (50 mM Tris·HCl, 10 mM $MgCl_2$, 125 mM NaCl, 5 mM DTT, 0.1 µg/mL albumin, 1 mM ATP, pH 7.5) contained 0.75 µg of supercoiled pNO1 plasmid, 1.5 U of human DNA topoisomerase II, inhibitor, 1% DMSO and 0.008% Tween 20. Reaction mixtures were incubated at 37° C for 30 min. After that, the TF buffer (50 mM NaOAc, 50 mM NaCl and 50 mM $MgCl_2$, pH 5.0) was added and the mixtures were left for 30 min at RT, during which biotin-oligonucleotide–plasmid triplex was formed. The unbound plasmid was washed off with TF buffer. Then the solution of Diamond Dye in T10 buffer (10 mM Tris·HCl, 1 mm EDTA, pH 8.0) was added. After 15 min of incubation in the dark, fluorescence was measured with a microplate reader (BioTek Synergy H4, excitation: 485 nm, emission: 537 nm). Initial screening was done at 10 and 100 µM concentrations of inhibitors. As the positive control, etoposide (TCI, Tokyo, Japan; IC_{50} = 71 µM) was used.

5. Results & discussion

The synthesis of IMD-03 and IMD-04 was achieved through a multi-step synthesis. Starting from etherification of 4-(methylsulfonyl)-2-nitrophenol with a yield of 68 % (IMD-01) followed by reduction with iron in neat acetic acid with a yield of 96 % (IMD-02). The most important and most problematic step was the synthesis of IMD-03 itself. In this coupling reaction, a pyrrole acid was coupled with a primary aromatic amino group to form an amide bond. Based on knowledge and experience gained during previous research, the coupling was prepared by activation of the pyrrole carboxylic acid with thionyl chloride to the corresponding acyl chloride. The coupling reaction was unsuccessful and reaction conditions were changed. Toluene heated to 130° C under a condenser was used instead of DCM at room temperature. The yield of IMD-03 was 56 % followed by hydrolysis obtaining IMD-04. Reaction conditions of the hydrolysis had to be changed (increasing temperature to 70 °C) to earn a yield of 58 %. There were struggles with poor solubility during the synthesis of the substances, especially IMD-03 and IMD-04. Introducing IBI-06 into the molecule dramatically increased lipophilicity because of dichlorinated aromatic heterocyclic moiety and thus impaired solubility. For HPLC-MS analysis of these compounds, a different sample preparation approach, where the compound was dissolved in DMSO, has been used.

Synthesis of variation with benzothiazole instead of methylsulfonyl group was attempted in the IMD 1 series. Unfortunately, these reactions failed during the reduction step after the creation of a benzothiazole ring with thiocyanate and bromine (creation of IMD-12). IMD-12 was insoluble (even in boiling DMSO). NMR was done, but it was inconclusive because of very weak signals. It was decided to proceed to the next step anyway. The reaction mixture from the reduction was impossible to separate, so this series was abandoned.

For the last series of compounds, the starting material was prepared from a fluorinated compound. Fluorine is usually classified as a poorly leaving group. However, nucleophilic aromatic substitutions with fluorine as the leaving group were discovered to be 3300 times faster than reactions with iodine in some cases.[47] The high electronegativity of fluorine atoms causes pulling electron density out of the ring activating it to attack. The position for substitution was determined by the position of the leaving group.[48]

IMD-22 was synthesized in great amounts and then it was put into reaction with three different compounds. In the first attempts during reactions with all three variations, the same peak occurred in the HPLC-MS spectrum. The impurity had its origins in impure DMF, for the second attempt ACN was chosen as the solvent. The slow course of the IMD-23 reaction was probably caused by a steric block of the reagents.

IMD-03 was tested against hTopoII alpha on relaxation assay. Its preliminary IC_{50} is 25 μM. In comparison, previously synthesized compounds by Skok et al. with great on-target activity had IC_{50} between 0.6 – 10 μM. On the other hand, some compounds synthesized in previous studies with great on-target activity were very weakly cytotoxic or did not possess cytotoxicity at all. They also were non-selective to hTopoII isoform α.[31,45] Therefore it is important to do further biological testing. One of the reasons for poor on-target activity can be the poor solubility of synthesized compounds. This property makes them hard to work with. Skok et al. were facing the problem of poor solubility as well.

6. Conclusion

In total, twelve compounds were prepared during the project. Two of them being final compounds (not previously published) and ten being reaction intermediates. Five more compounds are yet to be finished.

Certainly, further progress is needed, such as finishing the IMD-2 series and evaluating inhibitory activity to hTopoIIα. This work expanded the library of ATP-competitive inhibitors; however, activity and physicochemical properties remain unimproved.

There are numerous limitations in cancer therapy, lack of selectivity is a remarkable one. There will be prepared more derivatives of the binding motive described in Figure 1 with better physicochemical properties as well as with improved selectivity to the α isoform of human topoisomerase II.

7. Literature

1. Ferlay J, Colombet M, Soerjomataram I, et al. Cancer statistics for the year 2020: An overview. *Int J Cancer*. 2021;149(4):778-789. doi:10.1002/ijc.33588

2. Cancer. Accessed March 12, 2023. https://www.who.int/health-topics/cancer#tab=tab_1

3. Jemal A, Bray F, Center MM, Ferlay J, Ward E, Forman D. Global cancer statistics. *CA Cancer J Clin*. 2011;61(2):69-90. doi:10.3322/caac.20107

4. Ferlay J, Colombet M, Soerjomataram I, et al. Estimating the global cancer incidence and mortality in 2018: GLOBOCAN sources and methods. *Int J Cancer*. 2019;144(8):1941-1955. doi:10.1002/ijc.31937

5. Muresanu C, Khalchitsky S. Updated Understanding of the Causes of Cancer, and a New Theoretical Perspective of Combinational Cancer Therapies, a Hypothesis. *DNA Cell Biol.* 2022;41(4):342-355. doi:10.1089/DNA.2021.1118

6. IARC History – IARC. Accessed March 12, 2023. https://www.iarc.who.int/iarc-history/

7. Khan YS, Farhana A. Histology, Cell. *StatPearls*. Published online May 1, 2023. Accessed May 2, 2023. https://www.ncbi.nlm.nih.gov/books/NBK554382/

8. Wong RSY. Apoptosis in cancer: From pathogenesis to treatment. *J Exp Clin Cancer Res*. 2011;30(1):87. doi:10.1186/1756-9966-30-87

9. Jakóbisiak M, Lasek W, Gołąb J. Natural mechanisms protecting against cancer. *Immunol Lett*. 2003;90(2-3):103-122. doi:10.1016/j.imlet.2003.08.005

10. Loose D, Van De Wiele C. The immune system and cancer. *Cancer Biother Radiopharm*. 2009;24(3):369-376. doi:10.1089/CBR.2008.0593

11. What Is Cancer? - NCI. Accessed March 25, 2023. https://www.cancer.gov/about-cancer/understanding/what-is-cancer

12. Cancer | Stanford Health Care. Accessed March 25, 2023. https://stanfordhealthcare.org/en/medical-conditions/cancer/cancer.html

13. Papalazarou V, Maddocks ODK. Supply and demand: Cellular nutrient uptake and exchange in cancer. *Mol Cell*. 2021;81(18):3731-3748. doi:10.1016/J.MOLCEL.2021.08.026

14. Salerno S, Da Settimo F, Taliani S, et al. Recent advances in the development of dual topoisomerase I and II inhibitors as anticancer drugs. *Curr Med Chem*. 2010;17(35):4270-4290. doi:10.2174/092986710793361252

15. Vosberg HP. DNA topoisomerases: enzymes that control DNA conformation. *Curr Top Microbiol Immunol*. 1985;114:19-102. doi:10.1007/978-3-642-70227-3_2

16. Champoux JJ. DNA topoisomerases: Structure, function, and mechanism. *Annu Rev Biochem*. 2001;70:369-413. doi:10.1146/ANNUREV.BIOCHEM.70.1.369

17. How does prokaryotic DNA supercoil into its tertiary structure? Accessed April 7, 2023. https://www.brainkart.com/article/How-does-prokaryotic-DNA-supercoil-into-its-tertiary-structure-_27536/

18. 7.2B: Supercoiling - Biology LibreTexts. Accessed April 7, 2023. https://bio.libretexts.org/Bookshelves/Microbiology/Microbiology_(Boundless)/07%3A_Microbial_Genetics/7.02%3A_Prokaryotic_Genomes/7.2B%3A_Supercoiling

19. Witz G, Stasiak A. DNA supercoiling and its role in DNA decatenation and unknotting. *Nucleic Acids Res*. 2010;38(7):2119-2133. Doi:10.1093/NAR/GKP1161

20. Baranello L, Levens D, Gupta A, Kouzine F. The importance of being supercoiled: how DNA mechanics regulate dynamic processes. *Biochim Biophys Acta*. 2012;1819(7):632-638. doi:10.1016/J.BBAGRM.2011.12.007

21. Vologodskii A. Unlinking of Supercoiled DNA Catenanes by Type IIA Topoisomerases. *Biophys J*. 2011;101(6):1403-1411. doi:10.1016/J.BPJ.2011.08.011

22. Pommier Y, Nussenzweig A, Takeda S, Austin C. Human topoisomerases and their roles in genome stability and organization. *Nat Rev Mol Cell Biol*. 2022;23(6):407-427. doi:10.1038/s41580-022-00452-3

23. Pommier Y. Drugging topoisomerases: Lessons and Challenges. *ACS Chem Biol*. 2013;8(1):82-95. doi:10.1021/CB300648V

24. Collin F, Karkare S, Maxwell A. Exploiting bacterial DNA gyrase as a drug target: current state and perspectives. *Appl Microbiol Biotechnol*. 2011;92(3):479-497. doi:10.1007/S00253-011-3557-Z

25. Ahmad M, Xu D, Wang W. Type IA topoisomerases can be "magicians" for both DNA and RNA in all domains of life. *RNA Biol*. 2017;14(7):854-864. doi:10.1080/15476286.2017.1330741

26. Baker NM, Rajan R, Mondragń A. Structural studies of type I topoisomerases. *Nucleic Acids Res*. 2009;37(3):693-701. doi:10.1093/NAR/GKN1009

27. Delgado JL, Hsieh CM, Chan NL, Hiasa H. Topoisomerases as anticancer targets. *Biochem J*. 2018;475(2):373-398. doi:10.1042/BCJ20160583

28. Larsen AK, Escargueil AE, Skladanowski A. Catalytic topoisomerase II inhibitors in cancer therapy. *Pharmacol Ther*. 2003;99(2):167-181. doi:10.1016/S0163-7258(03)00058-5

29. Nitiss JL. DNA topoisomerase II and its growing repertoire of biological functions. *Nat Rev Cancer*. 2009;9(5):327-337. doi:10.1038/nrc2608

30. Van Ravenstein SX, Mehta KP, Kavlashvili T, et al. Topoisomerase II poisons inhibit vertebrate DNA replication through distinct mechanisms. *EMBO J*. 2022;41(12):E110632. doi:10.15252/EMBJ.2022110632

31. Skok Ž, Durcik M, Gramec Skledar D, et al. Discovery of new ATP-competitive inhibitors of human DNA topoisomerase IIα through screening of bacterial topoisomerase inhibitors. *Bioorg Chem*. 2020;102:104049. doi:10.1016/J.BIOORG.2020.104049

32. Vann KR, Oviatt AA, Osheroff N. Topoisomerase II Poisons: Converting Essential Enzymes into Molecular Scissors. *Biochemistry*. 2021;60(21):1630-1641. doi:10.1021/ACS.BIOCHEM.1C00240

33. Pommier Y. Topoisomerase I inhibitors: camptothecins and beyond. *Nat Rev Cancer*. 2006;6(10):789-802. doi:10.1038/nrc1977

34. Martino E, Della Volpe S, Terribile E, et al. The long story of camptothecin: From traditional medicine to drugs. *Bioorg Med Chem Lett*. 2017;27(4):701-707. doi:10.1016/j.bmcl.2016.12.085

35. Talukdar A, Kundu B, Sarkar D, Goon S, Mondal MA. Topoisomerase I inhibitors: Challenges, progress and the road ahead. *Eur J Med Chem*. 2022;236:114304. doi:10.1016/J.EJMECH.2022.114304

36. Li Z, Li X, Cao Z, et al. Camptothecin nanocolloids based on N,N,N-trimethyl chitosan: Efficient suppression of growth of multiple myeloma in a murine model. *Oncol Rep*. 2012;27(4):1035-1040. doi:10.3892/OR.2012.1635

37. Nitiss JL. Targeting DNA topoisomerase II in cancer chemotherapy. *Nat Rev Cancer*. 2009;9(5):338-350. doi:10.1038/NRC2607

38. Pendleton M, Lindsey RH, Felix CA, Grimwade D, Osheroff N. Topoisomerase II and leukemia. *Ann N Y Acad Sci*. 2014;1310(1):98-110. doi:10.1111/NYAS.12358

39. Matias-Barrios VM, Radaeva M, Song Y, et al. Discovery of New Catalytic Topoisomerase II Inhibitors for Anticancer Therapeutics. *Front Oncol*. 2021;10:633142. doi:10.3389/FONC.2020.633142

40. Skok Ž, Zidar N, Kikelj D, Ilaš J. Dual Inhibitors of Human DNA Topoisomerase II and Other Cancer-Related Targets. *J Med Chem*. 2020;63(3):884-904. doi:10.1021/ACS.JMEDCHEM.9B00726

41. Jirkovský E, Jirkovská A, Bavlovič-Piskáčková H, et al. Clinically Translatable Prevention of Anthracycline Cardiotoxicity by Dexrazoxane Is Mediated by Topoisomerase II Beta and Not Metal Chelation. *Circ Heart Fail*. 2021;14(11):E008209. doi:10.1161/CIRCHEARTFAILURE.120.008209

42. Bailly C. Contemporary challenges in the design of topoisomerase II inhibitors for cancer chemotherapy. *Chem Rev*. 2012;112(7):3611-3640. doi:10.1021/CR200325F

43. Zidar N, Montalvão S, Hodnik Ž, et al. Antimicrobial Activity of the Marine Alkaloids, Clathrodin and Oroidin, and Their Synthetic Analogues. *Mar Drugs*. 2014;12(2):940-963. doi:10.3390/MD12020940

44. Lu J, Patel S, Sharma N, et al. Structures of kibdelomycin bound to Staphylococcus aureus GyrB and ParE showed a novel U-shaped binding mode. *ACS Chem Biol*. 2014;9(9):2023-2031. doi:10.1021/CB5001197

45. Skok Ž, Durcik M, Zajec Ž, et al. ATP-competitive inhibitors of human DNA topoisomerase IIα with improved antiproliferative activity based on N-phenylpyrrolamide scaffold. *Eur J Med Chem*. 2023;249:115116. doi:10.1016/J.EJMECH.2023.115116

46. Juillard J. Dimethylformamide: Purification, Tests for Purity and Physical Properties. *Pure and Appl Chem*. 1977;49(6):885-892. doi:10.1351/PAC197749060885

47. Shortridge RW, Craig RA, Greenlee KW, et al. The "Element Effect" as a Criterion of Mechanism in Activated Aromatic Nucleophilic Substitution Reactions. *J Am Chem Soc*. 1957;79(2):385-391. doi:10.1021/JA01559A040

48. Nucleophilic Aromatic Substitution: Introduction and Mechanism. Accessed August 27, 2023. https://www.masterorganicchemistry.com/2018/08/20/nucleophilic-aromatic-substitution-nas/